

A multiscale modeling framework for studying the mechanobiology of sarcopenic obesity

Naama Shoham¹ · Ayelet Levy¹ · Nogah Shabshin^{2,3} · Dafna Benayahu⁴ · Amit Gefen¹

Received: 15 April 2016 / Accepted: 8 August 2016 / Published online: 16 August 2016
© Springer-Verlag Berlin Heidelberg 2016

Abstract An inactive sedentary lifestyle is a common risk factor contributing to sarcopenic obesity. At the cell scale, sustained mechanical deformations of the plasma membrane (PM) in adipocytes, characterizing chronic static loading in weight-bearing tissues during prolonged sitting or lying, were found to promote adipogenesis. Taking a mechanobiological perspective, we correlated here the macroscale mechanical deformations of weight-bearing adipose tissues (subcutaneous and intramuscular) with mechanical strains developing in the PMs of differentiating adipocytes. An innovative multiscale modeling framework for adipose tissues was developed for this purpose, where the buttocks, adipose tissues, adipocytes and the subcellular components: intracytoplasmic nucleus and lipid droplets as well as the PMs of the cells, were all represented. We found that a positive feedback loop very likely exists and is involved in the onset and progression of sarcopenic obesity, as follows. Adipogenesis in statically deformed adipocytes results in gaining more macroscopic subcutaneous and intramuscular fat mass, which then increases fat deformations macroscopically and microscopically, and hence triggers additional adipogenesis, and so on. Our present study is highly relevant in research of

sarcopenic obesity and other adipose-related diseases such as diabetes, since mechanical distortion of adipocytes promotes adipogenesis and fat gain at the different dimensional scales.

Keywords Adipose tissue · Adipogenesis · Mechanotransduction · Finite element model

1 Introduction

Aging of populations and weight gain up to morbid obesity are two well-recognized trends nowadays, in both developed and developing countries. Age-related loss of muscle mass, i.e., sarcopenia, affects approximately one-third of the adults over 60 years of age and more than 50% of those over 80 years (Parr et al. 2013; Roubenoff 2004). In addition, more than 50% of the adult population in the USA is expected to be obese by 2030 (Finkelstein et al. 2012). Sedentary lifestyle is a commonly described risk factor contributing to both sarcopenia and obesity. Daily physical activity is essential for mesenchymal stem cells (MSC) positioned in intramuscular fat (IF) within skeletal muscle tissues to differentiate into myoblasts rather than adipocytes (Santilli et al. 2014; Stenholm et al. 2008; Vettor et al. 2009). Indeed, during immobilization periods in the order of several weeks, or in chronic immobilization such as after an injury to the central nervous system, these MSCs will tend to follow an adipogenic fate, which will eventually increase the mass of IF depots (Gefen 2014; Ivanovska et al. 2015; Shefer et al. 2010). In addition, physical exercise that increases the energy expenditure component of the body energy balance is known for decades to contribute to loss of fat mass (Benton et al. 2011; Goisser et al. 2015; Parr et al. 2013; Vettor et al. 2009). Recent research points to a mechanotransduction effect influencing the differentiation fate of MSCs and

✉ Amit Gefen
gefen@eng.tau.ac.il

¹ Department of Biomedical Engineering, Faculty of Engineering, Tel Aviv University, 69978 Tel Aviv, Israel

² Department of Radiology, Haemek Medical Center, Afula, Israel

³ Department of Radiology, Hospital of University of Pennsylvania, Philadelphia, PA, USA

⁴ Department of Cell and Developmental Biology, Sackler School of Medicine, Tel Aviv University, Tel Aviv, Israel

suppressing selection of the adipogenic phenotype (Delaine-Smith and Reilly 2012). The coexistence of sarcopenia and obesity, called *sarcopenic obesity*, is characterized by marked weakness of the affected muscles as a result of loss of tissue mass, and as (noncontractile) fat depots expand. Each of the individual conditions, obesity and sarcopenia, can elevate morbidity and mortality. Obesity may lead to cardiovascular events or cerebrovascular accidents, and sarcopenia may lead to falls and hip fractures. The confluence of these two conditions in sarcopenic obesity, however, is even more dangerous, due to the synergistic nature of the comorbidities, particularly the mutual effects on the endocrine system and blood chemistry (Roubenoff 2004; Santilli et al. 2014; Zamboni et al. 2008). For example, the loss of muscle reduces the mass of available insulin-responsive target tissues and hence promotes insulin resistance, which, in turn, stimulates the metabolic syndrome and obesity, as well as hyperglycemia which leads to type-2 diabetes. In addition, an increase in the fat mass promotes production of tumor necrosis factor- α , interleukin-6, and other adipokines that not only amplify the insulin resistance but also have direct catabolic effect on muscle tissues (Roubenoff 2004).

Clinical studies reveal that fat distribution and metabolic influence vary by gender, race, and health conditions (Goodpaster et al. 2000, 2005; Albu et al. 2005, 2007; Yim et al. 2007, 1985; Robles et al. 2015). In lean and obese glucose-tolerant subjects and in obese subjects with diabetes mellitus, for example, a negative association between IF tissues and insulin sensitivity was found (Goodpaster et al. 2000). The same research group also found that high-IF tissue was significantly associated with the metabolic syndrome in normal-weight and overweight subjects, but not in obese subjects (Goodpaster et al. 2005). Interestingly, in African-American women, higher-IF tissue was found to be an independent predictor of lower insulin sensitivity at a greater extent than in Caucasian nondiabetic women (Albu et al. 2005). In later studies, IF tissue in healthy adults and in HIV+ women was found to have a strong independent association with fasting glucose levels (Yim et al. 2007) and insulin resistance (Albu et al. 2007), respectively. In the study of Yim et al. (1985), femoral–gluteal IF tissue was significantly associated with glucose level, independent of visceral adipose tissue mass. Moreover, regional fat varied between races so that Asian women had less femoral–gluteal subcutaneous adipose tissues and African-American and Asian men had greater femoral–gluteal IF tissue. Patients with chronic obstructive pulmonary disease were examined in the study of Robles et al. (2015), where significantly greater lipid accumulation and muscle atrophy were documented in people with the disease than in their healthy counterparts. The increased intramuscular fat infiltration has a stronger correlation with muscle weakness and impaired mobility than the muscle size.

Current lifestyle interventions to treat sarcopenic obesity include adoption of an exercise program (Benton et al. 2011; Goisser et al. 2015; Parr et al. 2013; Shefer et al. 2010). One of the reasons for exercise to be considered a remedy for sarcopenic obesity is that physiological dynamic activities trigger mechanoreceptors in bone and muscle cells, which in turn modulate the production of growth factors that stimulate muscle cell and tissue growth (Velloso 2008). Nevertheless, the responsiveness of adipocytes positioned in the intramuscular fat depots to mechanical stimuli was not addressed in the context of sarcopenic obesity.

Adipocytes are currently becoming recognized as mechanosensitive cells, as demonstrated experimentally by our group and others by means of cell culture models, animal studies and human trials. Overall, dynamic mechanical loads such as cyclic stretching at physiological rates characterizing physical exercise were found to suppress adipogenesis and to decrease fat mass. Sustained mechanical stretching, however, characterizing chronic static loading in weight-bearing tissues during prolonged sitting or lying, was found to have the opposite effect, that is, it promoted and accelerated adipogenesis (Case et al. 2013; Kato et al. 2010; Khouri et al. 2000; Krishnamoorthy et al. 2016; Levy et al. 2012; Li et al. 2013a, 2015; Luu et al. 2009; Rubin et al. 2007; Shoham and Gefen 2012b; Shoham et al. 2012, 2015a; Tanabe et al. 2004; Turner et al. 2008; Yang et al. 2012). Cell culture studies have specifically demonstrated that deformations applied to the plasma membrane (PM) in adipocytes activate signaling pathways that regulate adipogenesis such as the MEK or the TGF β /Smad pathways (Levy et al. 2012; Shoham and Gefen 2012b; Shoham et al. 2012; Tanabe et al. 2004; Turner et al. 2008).

A mechanobiological approach was employed in this study, connecting statically stimulated adipocytes to the pathogenesis of sarcopenic obesity. Our hypothesis was that the distortion of the PM in adipocytes at the buttocks is influenced by the level of intramuscular fat at the macroscale, and by the level of maturation of adipocytes at the microscale. The buttocks was chosen since the largest skeletal muscles in the body—the glutei—are located in it. Accordingly, the objective of the present study was to correlate macroscale mechanical deformations of weight-bearing adipose tissues (intra- as well as extra-muscular fat) with tensile mechanical strains developing in the PM of differentiating adipocytes.

1.1 Multiscale modeling

Finite element (FE) modeling is a powerful research tool for evaluating organ-level deformations in fat tissues, coupled to the mechanical behavior of the individual, cellular building units of fat. Multiscale modeling (MSM) in computational biomechanics typically represents several hierarchies in the structure of the organs and tissues, where there are links for

exchange of information between these different hierarchical scales. As the goal of MSM is to simultaneously describe both macro- and microscale behaviors, homogenization is an important part of the methodology. Homogenization is the process of obtaining a macroscopic stress–strain response (i.e., effective material properties) from a material with a known heterogeneous microstructure, based on the concept of a representative volume element (RVE) which can be considered representative of the continuum. The RVE must be large enough to be statistically representative of the material microstructure, but it must still satisfy the continuum assumption that its dimensions are much smaller with respect to the macroscale dimensions. Typically in MSM, the deformation gradient tensor computed in the macroscale point is passed to the microscale RVE. Then, homogenization is performed using the deformation gradient coupled with suitable boundary conditions, and the resulting stress tensors are passed back to the macroscale (Reese et al. 2013). Developing conventional large deformation FE models of the entire (buttocks) with the fine details of cellular components requires huge, unfeasible computational resources and run times. Alternatively, here we took the feed-forward workflow approach originally introduced by Erdemir et al. (2015), where multiple models were used in a sequence.

MSM approaches were previously adopted in a wide range of biomechanical studies that were related to different tissues such as bone (Barkaoui et al. 2014; Colloca et al. 2014; Hambli et al. 2011), cartilage (Erdemir et al. 2015; Moo et al. 2012; Sibole and Erdemir 2012; Sibole et al. 2013; Tanska et al. 2015), ligaments (Reese et al. 2013), and blood cells and arteries (Hartmann 2010; Hayenga et al. 2011). Fat tissues, however, have never been addressed in multiscale computational studies, although fat mechanobiology in obesity and diabetes is expected to contribute to the pathology at all the dimensional scales. We have previously developed an initial FE model of multiple adipocytes embedded in an extracellular matrix (ECM), which are stimulated mechanically in a static regime (Shoham 2015b). The cell/ECM density in this model was low, however, compared to the dense arrangement of adipocytes which is seen in native fat tissue sections. In addition, only compression loading was simulated, even though during weight-bearing postures such as sitting and lying, the adipose tissues are exposed to compound tensile, shear, and compression loading. Additional two-dimensional FE models of the buttocks (Levy et al. 2013, 2014; Shoham 2015b) and mesoscale adipose tissue (Ben-Or Frank et al. 2015), as well as three-dimensional FE models of individual adipocytes (Katzengold et al. 2015; Or-Tzadikario and Gefen 2011) were developed, but none of these studies incorporated or linked all the relevant dimensional scales in one modeling platform. Hence, a direct estimation of the deformations in the PMs of the cells when the buttocks is being loaded was not conducted to date. Accordingly, an innovative MSM frame-

work for adipose tissue is presented here, where the buttocks, adipose tissues, adipocytes, and the subcellular components: intracytoplasmic nucleus and lipid droplets as well as the PM of the cells, are all being considered in the modeling (Fig. 1).

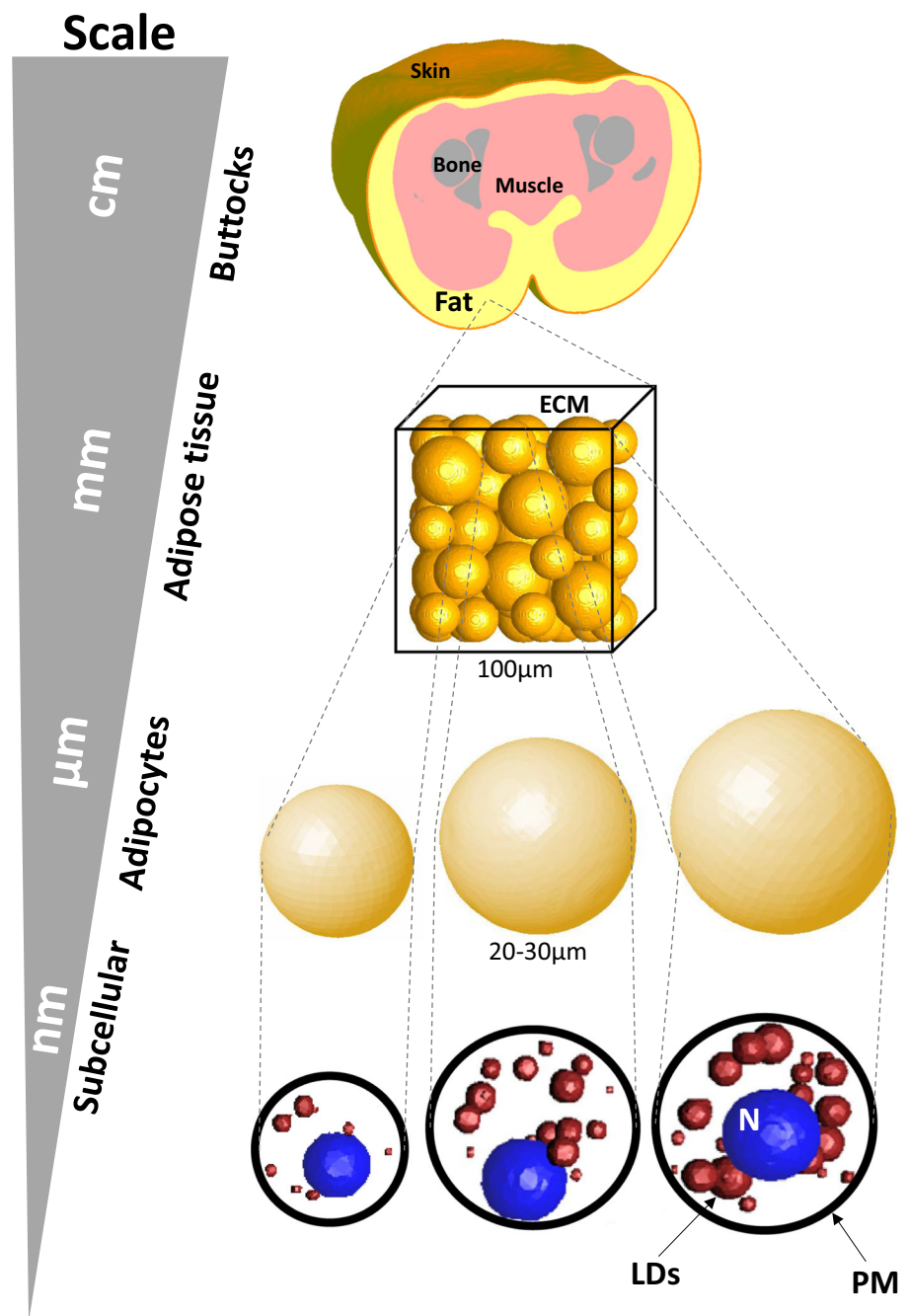
2 Methods

A novel three-dimensional (3D) multiscale finite element (FE) modeling framework for fat studies has been developed. We have used this new modeling framework for correlating macroscale mechanical loads in the adipose tissues of the buttocks with chronic microscale cell and subcellular deformations and the associated differentiation levels in adipocytes.

2.1 Macroscale modeling

A 3D large deformation FE model of the buttocks was developed based on sets of coronal supine MRI images, which were scanned by our group and were acquired from a 28-year-old healthy female subject (height = 1.66 m; weight = 57 kg). The imaging was performed in a 1.5-Tesla MR system (MAGNETOM Aera, SIEMENS AG, Munich, Germany) utilizing T1-weighted images (TR/TE = 550/10, field of view 420×420 mm, slice thickness 3 mm). The volunteer was lying on a custom-made support surface, specifically designed not to load the buttocks (Fig. 2a; upper frames). The MRI images of the nonweight-bearing (undeformed) buttocks were segmented using the ScanIP[®] module of the Simpleware[®] software package, in order to depict the different tissue components including bone, skeletal muscle, subcutaneous fat, and skin (Fig. 2b). Model dimensions were approximately $40 \times 30 \times 30$ cm³. A second comparable set of MRI images were taken from the same subject during full weight-bearing lying on a rigid support surface, in order to obtain the displacement boundary conditions of the sacrum, while it is sagging toward the surface (Fig. 2a; lower frame). The MRI study was approved by the Institutional Review Board (Helsinki Committee) of Assaf Horofeh Hospital (Approval no. 190/14). Two variant model configurations, with low and high intramuscular fat (IF) contents, were further generated (Fig. 3). Fat depots were virtually added within the muscle tissues as the subject was unrepresentative of the target sarcopenic obesity group. While we increased the fat mass between the low and high content configurations, it remains distributed throughout the muscle. The geometry of the fat infiltration patterns (but not the whole buttocks) was developed according to an MRI scan from individuals with IF tissue who were studied by our group in that context (Sopher et al. 2011). The muscle, fat, and skin tissues were modeled as nearly incompressible neo-Hookean solid hyperelastic materials, and the bones, as well

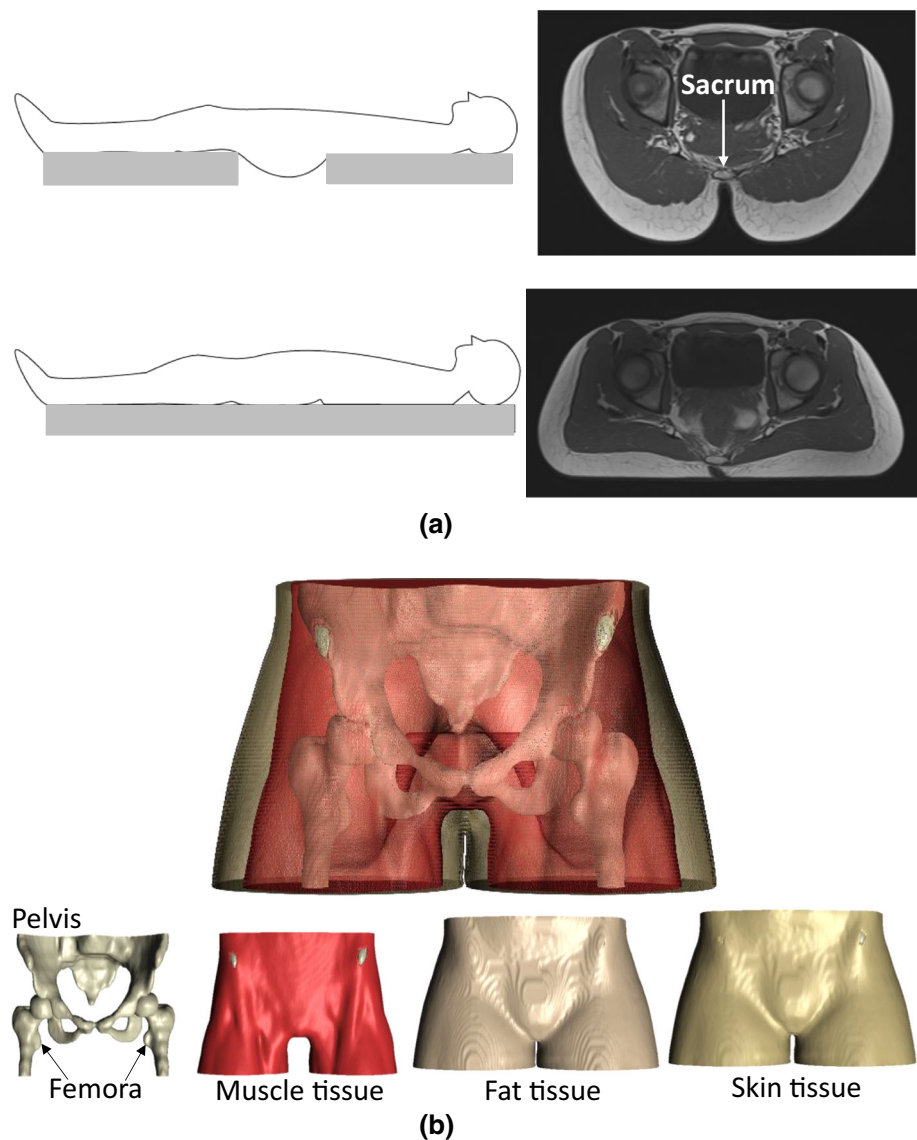
Fig. 1 The multiscale modeling framework for adipose studies, which included the buttocks, subcutaneous and intramuscular adipose tissues, adipocytes and the subcellular components: intracytoplasmic nucleus (N) and lipid droplets (LDs) as well as the plasma membrane (PM) of the cells. The cells are surrounded by extracellular matrix (ECM)



as a mattress which has been incorporated in the simulations (Fig. 1), were considered isotropic and linear elastic. The mechanical properties of bone, muscle, fat, and skin tissues (Table 1) have been adopted from Oomens et al. (2013), but were adjusted so that the deformations of the soft tissues during full weight-bearing showed the best fit to the anatomical data of the loaded MR scans which we have acquired as well from the same subject. The mechanical properties of the support were then set to fit commonly used support surfaces (Levy et al. 2013, 2014) (see Table 1), and an equivalent force of 90N, which caused the afore-

mentioned tissue deformations, was applied on the mattress. The boundary conditions included fixation of the lower surface of the mattress for all motion. Tied interfaces were set between all tissue components to allow feasible numerical solutions in this complex multiscale modeling framework since there are no relevant experimental data in the literature regarding the contact conditions (e.g., frictional sliding parameters) between the skin and subcutaneous soft tissues. Taking these considerations altogether, in practical terms, a tied interface seemed to be the optimal way forward. Frictional sliding was defined between the skin and the superior

Fig. 2 The process of tissues segmentation from magnetic resonance (MR) imaging. **a** Example MR images taken during non-weight bearing (undeformed) posture as the subject was lying on a custom-made support surface designed not to load the buttocks (upper frames), and during full weight-bearing (deformed) posture (lower frames). **b** Components of the buttocks model geometry, including the bone, skeletal muscle, fat and skin tissues



(contacting) surface of the mattress, with a friction coefficient of 0.4 (Levy et al. 2013, 2014). Tetrahedron and hexahedron elements were used to mesh the buttocks tissues and mattress, respectively. Due to the fact that the selected type of elements sometimes affect model predictions, we chose the same type of elements consistently in all models. Hence, our outcomes which are mainly comparative between all model variants could not have been substantially influenced by this chosen numerical technique. The numbers of mesh elements in the different components of the macroscale model variants are listed in Table 1. Convergence analyses showed that for a 12% denser mesh, the difference in average effective tissue strains was less than 1% for the same loading and other boundary conditions. All boundary conditions, constitutive laws and mechanical properties were defined using the PreView module of the FEBio software (version 1.14), and the model variants were analyzed using the FEBio FE

solver (<http://mrl.sci.utah.edu/software/febio>) in its structural mechanics mode.

2.2 Microscale modeling

Four variants of a 3D microscale model of fat tissue, including multiple adipocytes (52–94 cells), each with its unique intracellular structure, embedded in an extracellular matrix (ECM), were generated using an original, custom-made MATLAB code (Fig. 4). The dimensions of all these model variants were $100 \times 100 \times 100 \mu\text{m}^3$ of a tissue block. Each adipocyte included a cytoplasm that contained intracellular LDs and a nucleus. The sizes of the cells as well as the sizes and numbers of the lipid droplets (LDs) were set according to our previous experimental measurements in adipocyte cultures which undergo differentiation (Shoham and Gefen 2011; Shoham 2015b) (Table 2). We assumed mixed stage

Fig. 3 The macroscale geometries included a reference model, as well as low and high intramuscular fat content configurations

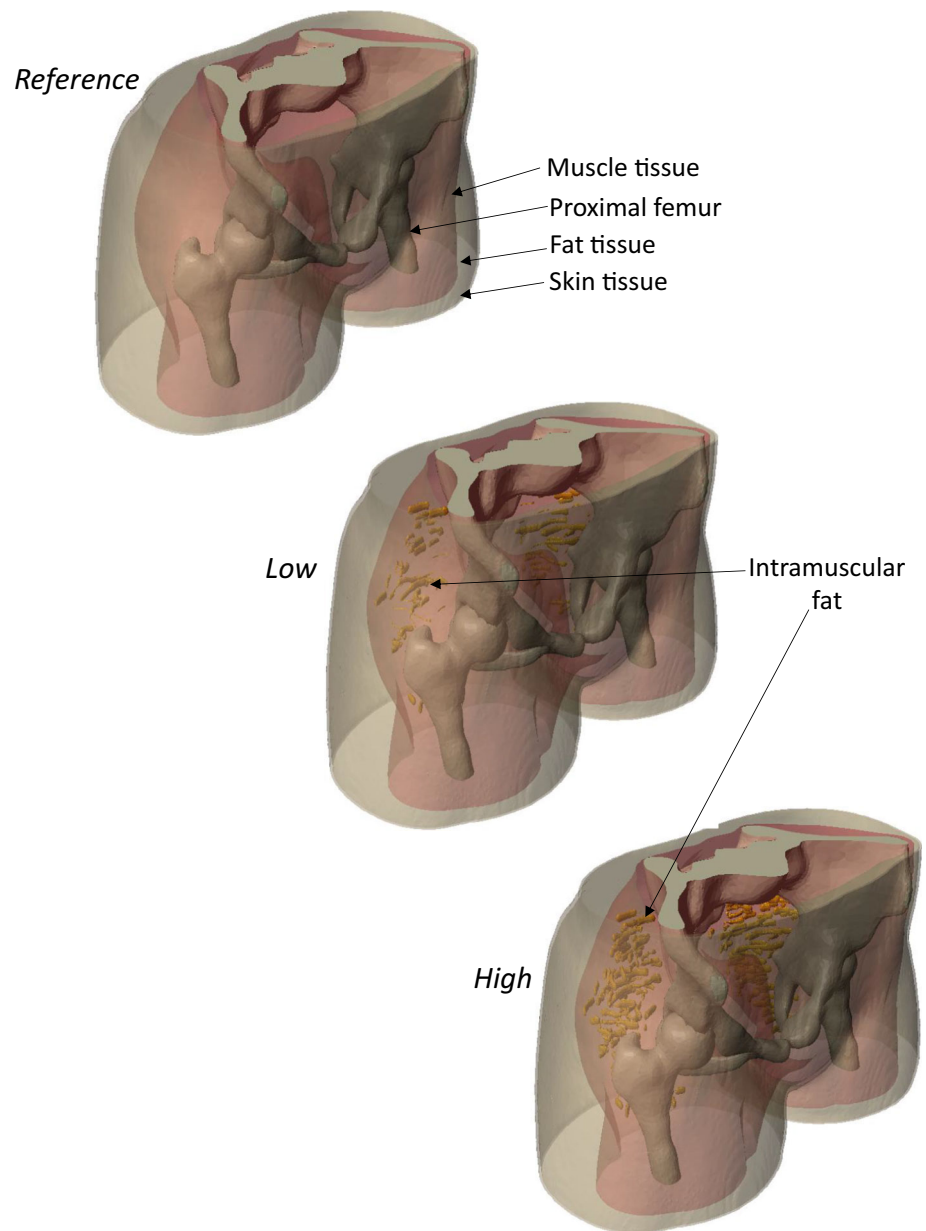


Table 1 Number of mesh elements and mechanical properties of the different components in the macroscale model

	Number of mesh elements			Mechanical properties	
	Reference	Mild FI	Severe FI	Elastic modulus [kPa]	Poisson's ratio
Skin	138,794	164,983	165,086	24	0.49
Fat	176,223	209,247	208,798	0.9	0.49
Muscle	123,191	651,021	625,671	3	0.49
Bone	42,835	47,796	47,674	7×10^6	0.3
Intramuscular fat	–	38,312	87,752	0.9	0.49
Mattress	36,000	36,000	36,000	30	0.3

FI fat infiltration

of maturity in each microscale model, which is realistic and which is the situation that we have observed in monolayer and in three-dimensional (tissue-engineered) adipocyte cul-

tures, as well as in histological analyses. Each adipocyte was assigned a different differentiation stage, which, for the purpose of the computational modeling, was defined as one of

Fig. 4 The microscale model variants of fat tissue, including multiple adipocytes, each with its unique intracellular structure, surrounded by extracellular matrix

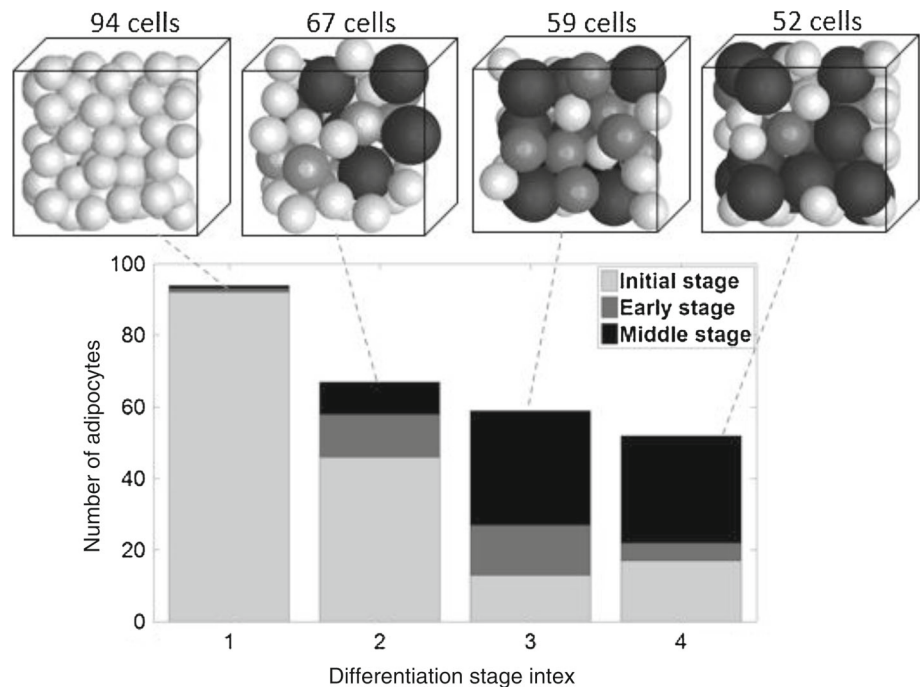


Table 2 Geometry parameters of the individual adipocytes embedded in the microscale model

Stage of differentiation	Initial	Early	Middle
Cell radius (μm)	9.6	11	11
LD radius (μm) (mean \pm SD)	4.87 \pm 0.70	6.55 \pm 0.74	6.81 \pm 0.56
Number of LDs (mean \pm SD)	4.83 \pm 1.89	18.00 \pm 8.97	20.89 \pm 5.02
Cell volume versus LD volume per cell (mean \pm SD)	186.2 \pm 53.54	41.48 \pm 27.98	15.90 \pm 3.98

LD lipid droplet, SD standard error

three possible stages: “initial,” “early,” or “middle” stage, in a stochastic manner. In culture differentiation stage (CDS) #3 model, for example, 13, 14, and 32 adipocytes were at an initial, early, and middle stage of differentiation, respectively. These initial, early, and middle stages represent adipocytes at days 5, 10, and 15 post-induction of differentiation, respectively, as shown in our published experimental work (Shoham and Gefen 2011). During their differentiation, adipocytes increase in size to allow accumulation of intracytoplasmic LDs. While the radii of these LDs consistently grow, their number first increases but then decreases as adjacent LDs fuse together to form fewer but larger droplets (Shoham et al. 2012). The positions of the adipocytes in the ECM, and of the LDs and nuclei intracellularly, were determined stochastically as well for their representation in the modeling, but the following constraints were applied: (1) Cells were forced to be attached to each other as seen in histology of native adipose tissues (Granneman et al. 2004) and (2) the nucleus, which occupied approximately 10 % of the total cell volume (Ben-Or Frank et al. 2015), was forced to be shifted toward the cell periphery in the adipocytes belonging to the “mid-

dle stage” group (Verstraeten et al. 2011). After setting the cell radius to be 9.6, 11, and 15 μm in the initial, early, and middle stage adipocytes, respectively, the sizes and numbers of LDs in each individual cell were raffled by the algorithm from the aforementioned empirically documented cell morphology data (Shoham and Gefen 2011), assuming normal statistical distributions of these parameters. The diversity in intracellular organization of each individual adipocyte realistically represented the cell-to-cell variability seen in both cultures and native tissue histology. Additional geometry parameters relevant to the microscale modeling including the mean cell and LD radii and the numbers of cells at each differentiation stage are provided in Tables 2 and 3, respectively. Each model variant was assigned a differentiation stage index (DSI) from #1 to 4, according to the mean cell radius, where the larger the mean cell radius was, the greater was the value of the index. Accordingly, a model with a higher DSI included adipocytes at a more advanced stage of differentiation, on average. All the model variants included adipocytes at the above-mentioned three differentiation stages (initial, early, and middle), but the number of cells at each stage changed

Table 3 Geometry and mesh parameters of the microscale models

	CDS #1	CDS #2	CDS #3	CDS #4
Total number of cells	94	67	59	52
Number of cells at an initial stage of differentiation	92	46	13	17
Number of cells at an early stage of differentiation	1	12	14	5
Number of cells at a middle stage of differentiation	1	9	32	30
Cell radius (μm) (mean \pm SD)	9.67 ± 0.57	10.57 ± 1.83	11.12 ± 2.16	11.5 ± 2.49
Number of ECM elements	580,836–1,005,073	463,124–729,104	556,364–823,264	419,275–1,312,021
Number of cytoplasm elements	1,745,046–1432552	1,274,176–1,489,969	1,360,842–1,557,951	58,124–1,208,525
Number of nucleus elements	62,631–71,076	52,192–60,307	61,455–70,850	48,880–1,477,035
Number of LD elements	70,535–70,740	111,540–112,396	127,266–131,410	129,404–135,910

CDS culture differentiation stage, SD standard error, ECM extracellular matrix, LD lipid droplet

between the models, as described in Table 3. The mean cell radius was 9.67 ± 0.57 , 10.57 ± 1.83 , 11.12 ± 2.16 , and $11.5 \pm 2.49 \mu\text{m}$ in DSI models #1, 2, 3, and 4, respectively. Considering maturation of individual adipocytes as a progress from initial, to early, and then to a middle stage of differentiation, adipose tissue maturation overall occurred from the DSI #1 to #4 microscale model variants. The plasma membrane of each cell was considered to be a thin layer in the cell periphery, with a width of $0.4 \mu\text{m}$, which was the minimum width that our Scan IP software was able to mesh. The cytoplasm (including the PM), nucleus, and LDs were assumed to behave according to a neo-Hookean strain energy density (SED) function, with a Poisson's ratio of 0.45 and elastic moduli of 0.77, 5, and 4.15 kPa, respectively, for these cell components (Table 4) (Shoham et al. 2014). The mechanical properties of the ECM was set according to the macroscale model, i.e., it was characterized by a neo-Hookean SED function with a Poisson's ratio of 0.49 and an elastic modulus of 0.9kPa (Table 1). The models were meshed with tetrahedron elements using the ScanIP[®] module of the Simpleware[®] software package. Convergence tests were conducted for the microscale modeling as well, and these yielded that a 30% denser mesh resulted in less than a 1.5% change in our outcome measures. The nodes on the faces of the tissue block model variants were prescribed displacement boundary conditions, u_i , which have been derived from the macroscale element deformation gradient tensors, F , as follows (Sibole and Erdemir 2012):

$$u_i = \sum_{j=1}^3 (F_{ij} X_j) - X_i \quad (1)$$

where X were the undeformed position vectors. After setting all the boundary conditions and mechanical properties in MATLAB, these models were run using the FEBio FE solver as well.

2.3 Protocol of simulation and outcome measures

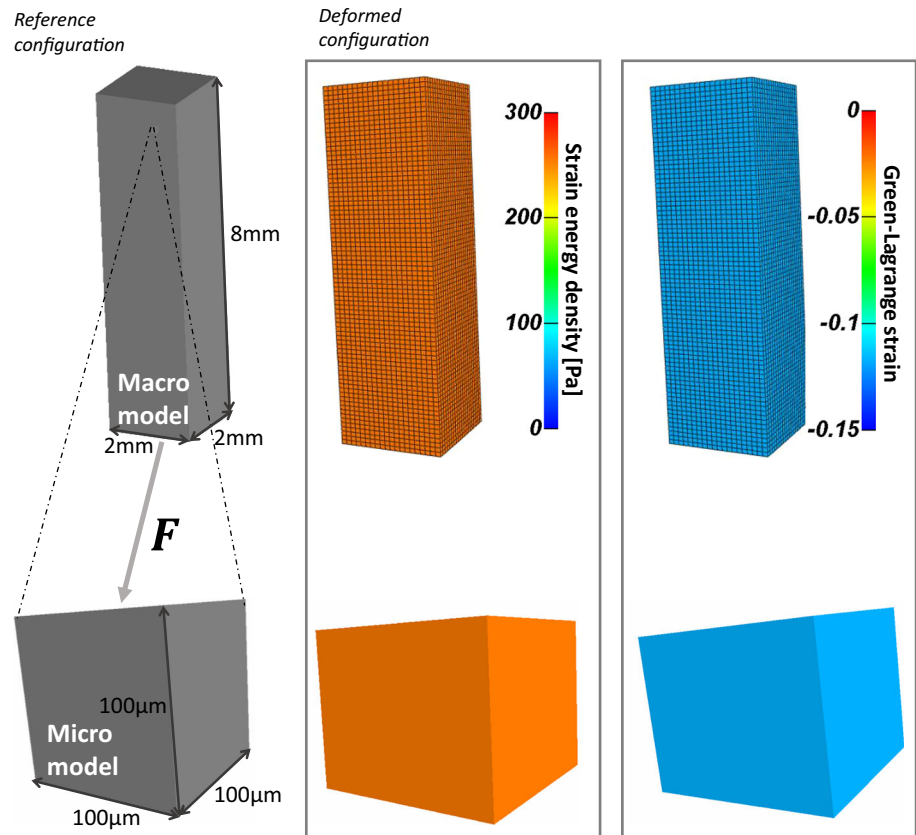
The effective strains which developed in the adipose tissues in the three macroscale model variants, i.e., in the reference, low, and high IF content configurations, were calculated both in the subcutaneous and in the intramuscular fat. Deformation gradient tensors calculated at centroids of three elements of interest in the reference model, which were positioned laterally and inferiorly at the coronal plane where the maximal strains occurred, were used for prescribing boundary conditions for each DSI microscale model variant (total of 12 runs). Two of these macroscale model elements, the lateral ones, were exposed to an effective Green–Lagrange strain of 30% and the third, inferior element was exposed to a strain of 60%. Tensile strains developing in the PMs of the adipocytes at the different differentiation stages were then examined as well, given the published empirical evidence that sustained exposure to such PM deformations would accelerate adipogenesis in cultures and in animal models (Levy et al. 2012; Shoham

Table 4 Mechanical properties of the different tissues in the microscale model

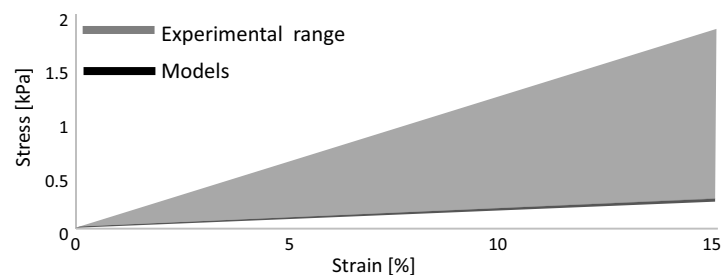
	ECM	Cytoplasm and plasma membrane	Nucleus	Lipid droplet
Elastic modulus (kPa)	0.9	0.77	5	4.15
Poisson's ratio	0.49	0.45	0.45	0.45

ECM extracellular matrix

Fig. 5 Validation of our multiscale approach: **a** Results from simple macro- and microscale models under compression with analytical solutions. The strain energy densities as well as the Green-Lagrange strains in the macro- and microscale models are provided in the upper and lower frames, respectively. **b** Comparison between the stress-strain behavior of the tissue block differentiation stage index (DSI) configurations and those of native subcutaneous human adipose tissues under tension tests. The gray area is the 70% confidence interval of the experimental results. The agreement is evident



(a)



(b)

and Gefen 2012b; Shoham et al. 2012, 2015a; Tanabe et al. 2004). The simulations were run on a 64-bit Windows 7-based workstation with an Intel Core i7 920 2.57 GHz CPU and 64GB of RAM. Runtimes for each multiscale problem (i.e., a coupled macro- and microvariant) ranged between 2 and 3 days, which were distributed so that computing the macroscale model variants took about 2 days and solving each microscale tissue block required 2–7 h.

2.4 Verification and validation

2.4.1 Verification of the multiscale approach

Simple macro- and microscale models of two boxes were developed for verification of our multiscale computational approach, by comparing it with analytical solutions (Fig. 5a). Specifically, an $8 \times 8 \times 2 \text{ mm}^3$ box was generated and meshed

with hexahedra in the PreView module of FEBio. The box was assumed to be made of an isotropic linear elastic material with an elastic modulus and a Poisson's ratio of 3 kPa and 0.49, respectively. The linear elastic material was chosen since it has the advantage of being described analytically. A simple compression test was then simulated by lowering the upper face of the box, and the Green–Lagrange strain and SED were calculated. We then ran a microscale simulation of a cube (facedimension = 100 μm), which was again developed and meshed with hexahedra in the PreView module of FEBio, applying the same linear elastic constitutive behavior and mechanical properties. Boundary conditions were applied according to Eq. 1 after calculating the deformation gradient tensor at a centroid of an element of interest at the macroscale box (Fig. 5a). The effective strain and the SED were uniform along the macroscale and microscale boxes, exactly as an analytical solution would indicate. Our custom-made MATLAB code for the above-mentioned multiscale approach was hence verified, given that the same values of Green-Lagrange strains and SED developed in both models (Fig. 5a).

2.4.2 Validation of the mechanical behavior of the microscale models

In order to verify that the mechanical behaviors of the microscale models were similar to that of native adipose tissues, the tissue block models were loaded in an unconfined tension mode and the resulted strain–stress curves were compared with the compressive response of human subcutaneous adipose tissues from the abdomen, which have been previously reported (Alkhouli et al. 2013). We found that the stress–strain curves obtained in our simulations for each tissue block were not influenced by the stage of maturity of the cells. Overall, the mechanical properties at each DSI were in good agreement with those of native subcutaneous human adipose tissues, though in the low range of the 70% confidence interval of such measurements (Fig. 5b) (Alkhouli et al. 2013). Our modeling data fall at the lower domain of the empirical results, likely because our models did not directly consider basement membrane structures within the ECM of adipose tissues, which would uncrimp and structurally restrain deformations under loading, thereby adding reinforcement and stiffness to the tissue blocks in real-world large deformation experiments. Nevertheless, the mean difference between the tangent moduli calculated from the linear portions of the modeling and mean experimental data curves (up to 15% strain) was 7%, which places the modeling data mildly above the lower limit of the empirical stress–strain data, but well within the empirical data range (Fig. 5b). Given the well-known issues of inter-specimen biological variability, tissue preservation, and testing method effects, we

consider the above as an adequate verification of our MSM framework.

3 Results

3.1 The macroscale models

An example comparison of strain distributions in subcutaneous and intramuscular adipose tissues, across the different macroscale models (i.e., the reference, low and high IF content configurations), for a supine posture, is provided in Fig. 6a (upper frames). In the reference configuration, where IF was not incorporated, the average effective strain in subcutaneous fat was 24%, with a relatively large spatial variability (standard deviation, SD, of 18%). The median and maximal strain values were 19 and 531%, respectively (Fig. 6c). The distortion of fat was hence considerably heterogeneous over the tissue volumes, with the greater strain values occurring in proximity to the sacrum, which is well expected based on previous modeling work (Linder-Ganz and Gefen 2004). Focusing now on the IF model configurations, the peak effective strain values within IF straps were 172 and 847% in the model variants with low and high IF contents, respectively (Fig. 6b). Consistently, muscle tissues were also distorted more in the high IF content configuration compared to the low IF configuration (Fig. 6a). This is likely due to larger shear strains occurring as a result of the sharp stiffness gradients between the interfacing (substantially more compliant; Table 1) fat straps and (stiffer) muscle tissues, where the IF contents were greater (Fig. 6a, lower frames). The subcutaneous adipose tissue covering the gluteus muscles was influenced by these elevated deformations as well, and so, the peak effective strain in subcutaneous fat increased from 198% in the low IF configuration to 257% in the high IF configuration. Overall, the magnitudes of the deformations that occurred in fat (both subcutaneous and intramuscular) increased substantially with the volume of the IF contents (Figs. 3, 6). When a larger number of IF straps were modeled (i.e., high IF contents), more fat tissue was positioned under and adjacent to the sacrum, and hence, the aforementioned muscle/fat stiffness gradient effect became more prominent. The elevated strains developing in the IF were then transferred to the muscle and the extra-muscular adipose tissues.

3.2 The microscale models

The deformations in PMs of adipocytes in the microscale models are provided in Figs. 7, 8. The microscale simulation data reported in Fig. 7 were divided into three groups, each corresponding to a different macroscale element. For convenience, these groups were termed here as “lateral left,” “lateral right,” and “inferior” simulations, according to the

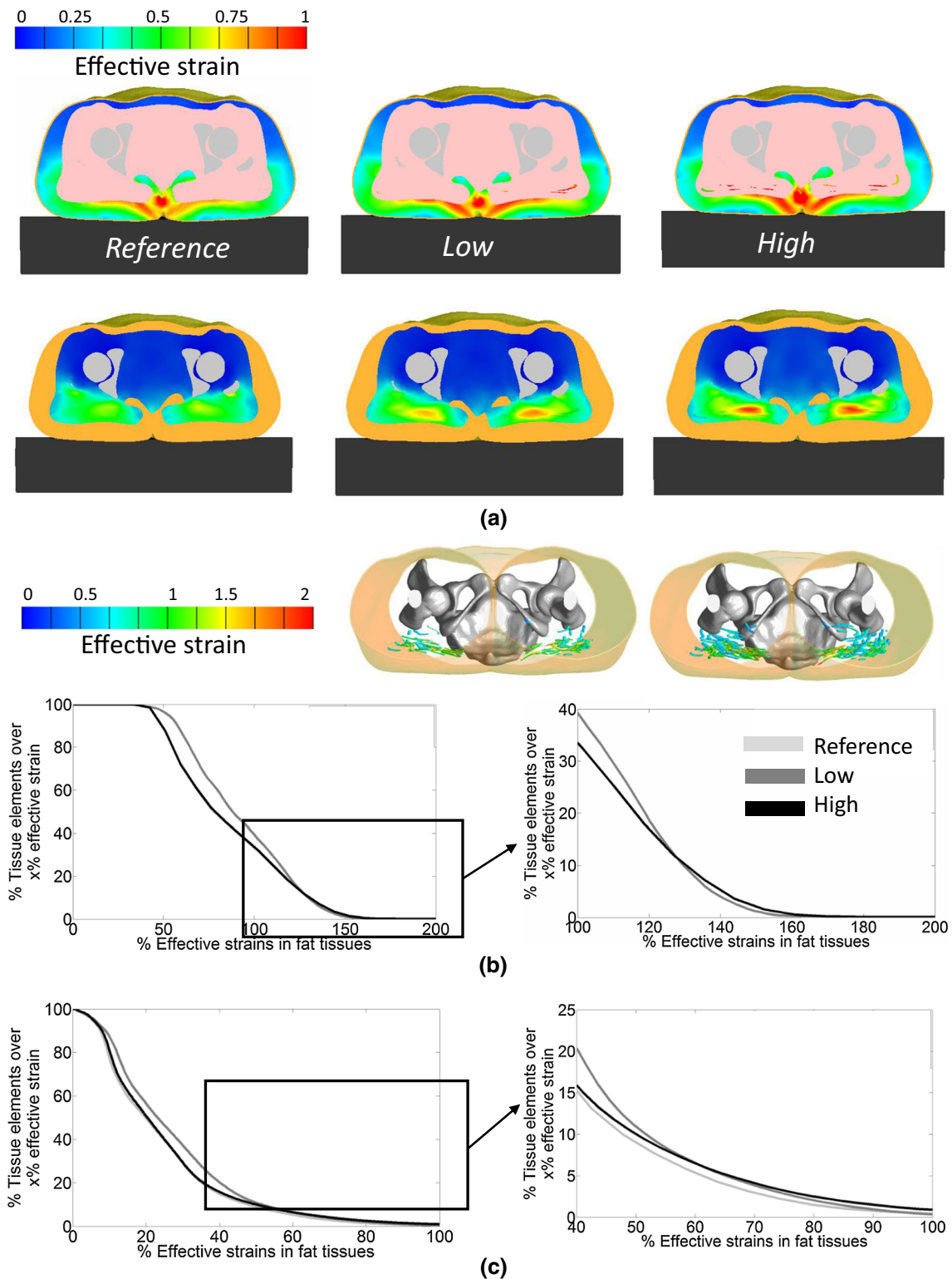


Fig. 6 a An example comparison between the distributions of the deformations developing in the intramuscular and subcutaneous adipose tissues (upper frames) and in the muscle (lower frames) in the

position of the individual elements in the cross-sectional view of the macroscale model of the supine buttocks. The levels of effective strains in the microscale models increased with

different macroscale model variants. Analyses of the effective strains in the intramuscular and subcutaneous fat are provided in panels **b** and **c**, respectively

the extent of localized deformations in the corresponding element at the macroscale model (Fig. 7). We did not find a substantial difference in the distortion of cells across the

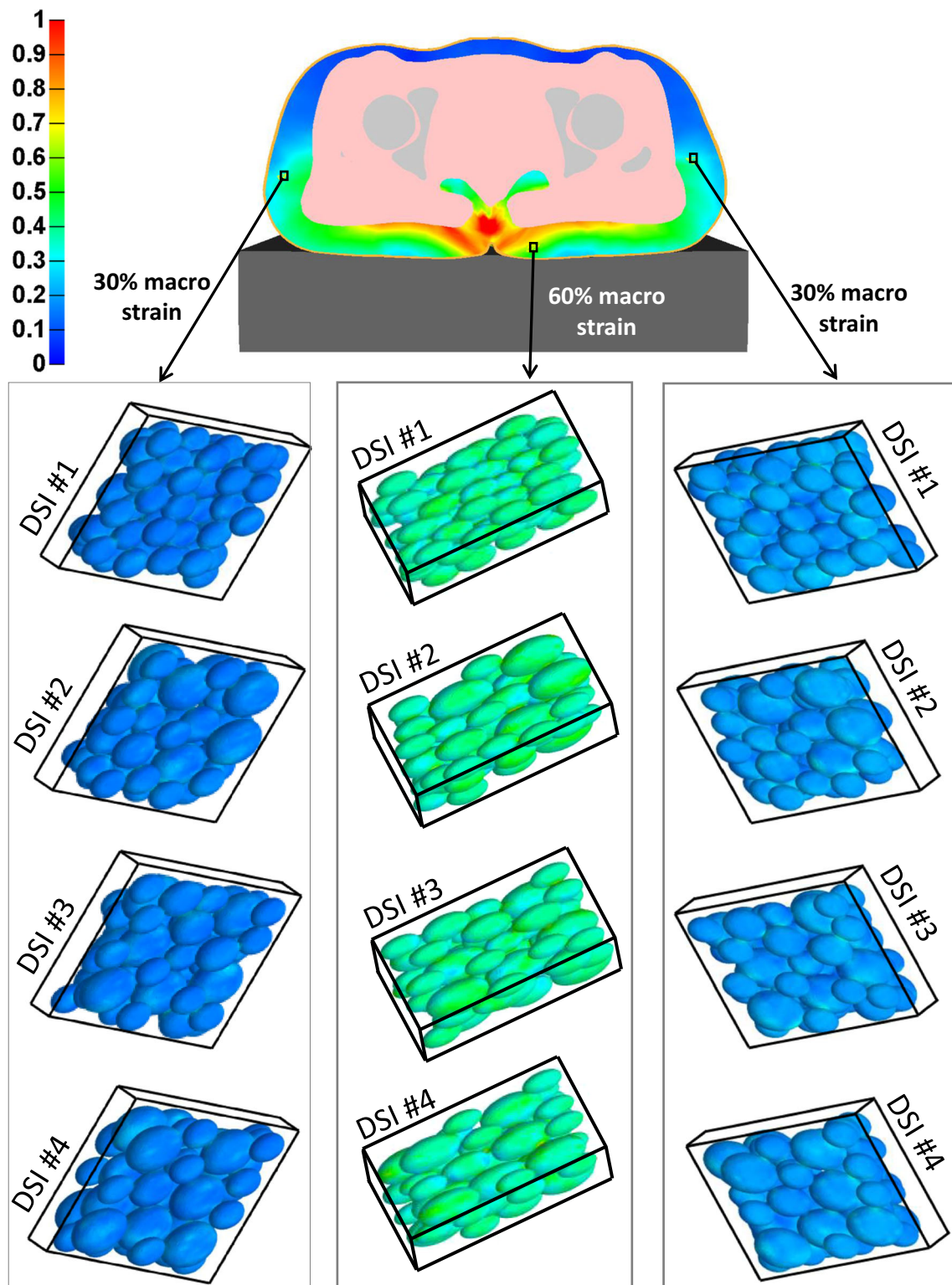


Fig. 7 The deformations developing in the plasma membrane of the adipocytes in the different differentiation stage index (DSI) microscale model configurations, divided into three groups, each corresponding to a different anatomical location (lateral/inferior) and macroscale element

DSI model variants (#1–4), per each simulation group (lateral right/left and inferior). In other words, deformations in the PMs of the studied adipocytes were *not* influenced by the

overall level of maturation of the adipose tissue block (Fig. 7). However, high deformations occurred in the PMs of the initial stage adipocytes, at their contact sites with neighboring

cells, and also in the PMs of the middle stage adipocytes—near large LDs (Fig. 8). The tensile strains developing in the PMs of the cells in the simulations attributed to the DSI #4 model variant at the “lateral left” location, for example, were 19 ± 4 , 20 ± 4 , and 21 ± 5 % (mean \pm SD) in the initial, early, and middle stage adipocytes, respectively (Fig. 8a). In another example, for the DSI #2 variant, and at the inferior location, effective strains were 45 ± 10 , 46 ± 10 , and 47 ± 11 % for the initial, early, and middle stage adipocytes (Fig. 8b). Hence, the PMs of the more mature adipocytes in each model were just slightly more distorted compared to those of the less mature cells (Figs. 8). In addition, the aforementioned data also show that the inhomogeneity in strain distributions increased as well, though moderately, with the level of differentiation of the individual adipocytes and the stage of differentiation of the tissue block.

Combining the results from the (linked) macro- and microscale models together, we conclude that the extent of deformations in the PMs of adipocytes increases with the level of IF contents. These elevated PM and cell strains are very likely to further stimulate differentiation and adipogenesis in the cells. Considering that the more mature cells are being more distorted compared to less mature ones, static loading of the buttocks in individuals with excessive IF contents should trigger further adipogenesis in a positive feedback loop.

4 Discussion

In this study, we present the first MSM of weight-bearing adipose tissues, spanning from the body level to a subcellular scale (Figs. 1, 7). Using this novel computational platform, we found that: (1) At the macroscale, adipose tissue deformations (both subcutaneous and intramuscular) increase with the amount of IF. (2) At the microscale, the magnitudes and inhomogeneity of deformations in the PMs of adipocytes increase with the level of cell maturation. Taken together, these two key findings indicate that excessive IF contents at the buttocks should lead to greater distortion of PMs in adipocytes when the buttocks are in sedentary weight-bearing postures, such as during prolonged sitting or lying. Based on extensive previous laboratory work published by our group and by others, it is reasonable to assume that PM receptors in fat cells would activate adipogenic signaling pathways under static loading, e.g., MEK/MAPK, as a result of exposure to these chronically static mechanical stimuli (Levy et al. 2012; Shoham and Gefen 2012b; Shoham et al. 2012; Shoham 2015b; Tanabe et al. 2004). Here, we describe a vicious cycle where adipogenesis in statically deformed adipocytes results in gaining more macroscopic subcutaneous and intramuscular fat mass, which increases fat deformations macroscopically and microscopically, hence

triggering and promoting additional adipogenesis, and so on (Elsner and Gefen 2008; Shoham et al. 2015a) (Fig. 9). This positive feedback loop is very likely involved in the onset and progression of sarcopenic obesity. The above description is the first mechanobiological perspective of the etiology of sarcopenic obesity, which is fundamentally important considering that mechanotransduction has been essentially ignored while previously describing this disease.

Our results at the macroscale are consistent with previous published studies, where IF inclusions were simulated in 2D slice models of the seated buttocks that were developed in the context of pressure ulcer research. The volumetric fractions of muscle and fat tissues that were exposed to elevated deformations in these sitting buttocks models increased with the growth in contents of IF (Shoham et al. 2015a; Sopher et al. 2011). We previously found that at a macroscopic scale, the loading state in the seated buttocks is considerably influenced by these changes, since skeletal muscle and adipose tissues have distinct stiffness properties (with muscle being much stiffer than fat), and hence, when the muscle–fat composition changes, tissue strain and stress magnitudes and distributions change as well (Elsner and Gefen 2008; Shoham et al. 2015a). This is consistent with the present work, though here the modeling was 3D, substantially more sophisticated and encompassed multiple dimensional scales, not just the whole buttocks scale. The extremely elevated localized strains occurred in the IF at the high IF content model in this study could lead to death of adipocytes, if being sustained, due to deformation damage, but this will likely be followed by cell renewal. Damage–repair cycles at the individual cell or cell group scales are to be expected, even in tissues with healthy fat contents, as part of the normal turnover process in fat; however, in subjects with excessive fat mass, there is often chronic inflammation in fat tissues, which may indeed relate to frequent cell deformation damage (Monteiro and Azevedo 2010; Gefen and Weihs 2016).

Our results at the microscale of the MSM framework are in agreement with our published findings from previous FE simulations of adipocytes, both isolated and in cultures (Ben-Or Frank et al. 2015; Katzungold et al. 2015; Or-Tzadikario and Gefen 2011; Shoham 2015b). Specifically, using 3D models of individual and groups of adipocytes embedded in ECM, which have been loaded in compression mode, we demonstrated that cells become structurally stiffer as they mature (Or-Tzadikario and Gefen 2011; Shoham et al. 2015a). Simulating single-cell mechanical compressing and stretching of adipocytes, Katzungold et al. (2015) showed that external loads induced localized effective strains in the PM which peaked over LDs, and this has been demonstrated in our models of tissue blocks with middle stage differentiated adipocytes as well. Additionally, previous mesoscale models of adipocytes in tissue-engineered constructs (at a sub-physiological density) revealed greater PM distortions

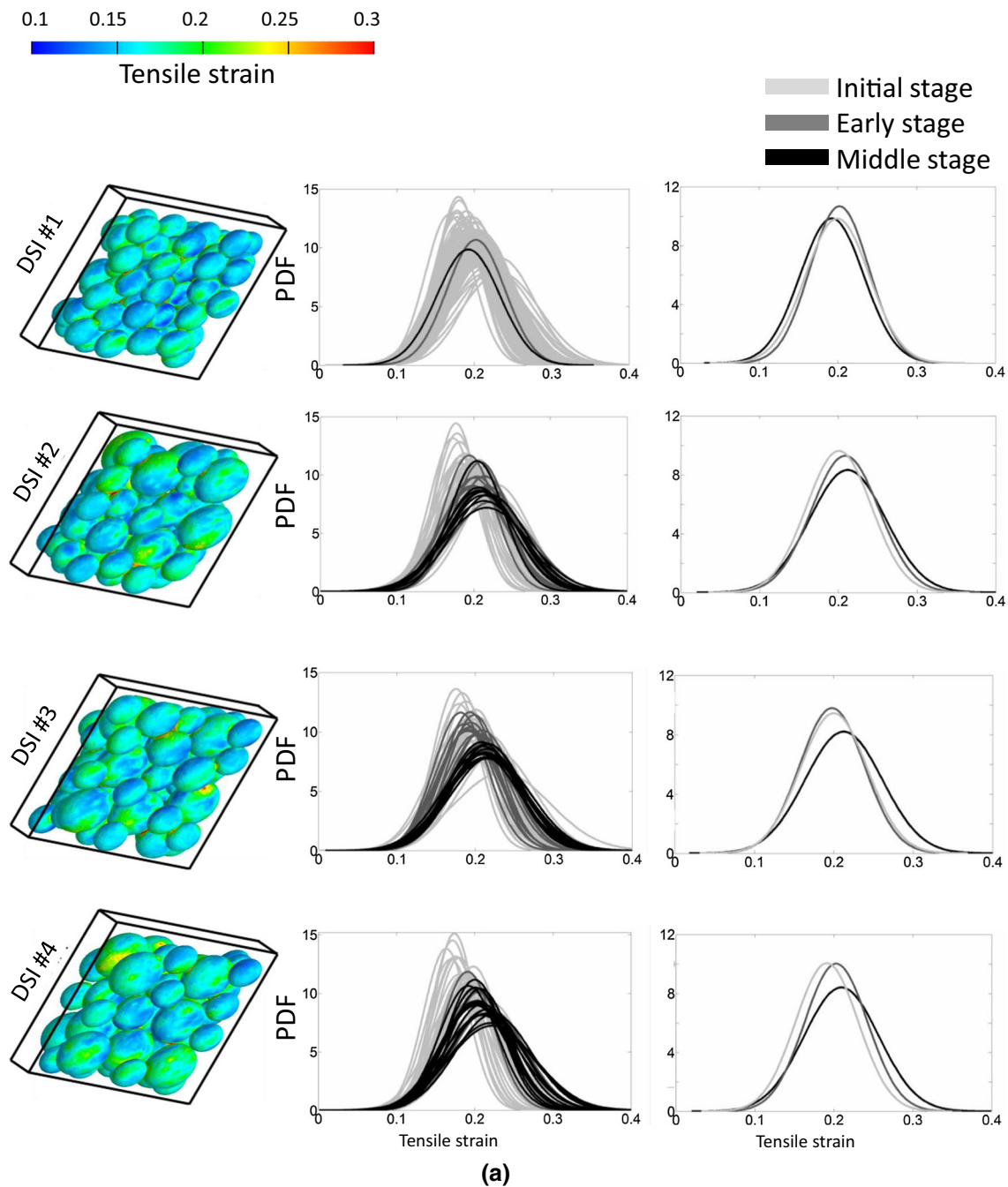


Fig. 8 Tensile strains developing in the plasma membrane of the adipocytes in the different differentiation stage index (DSI) microscale models, in the “lateral left” **a**, “inferior” **b** and “lateral right” **c** tissue blocks

in adipocytes following differentiation of neighboring cells in the loaded constructs (Shoham 2015b). This phenomenon was not reproduced in our present simulations, and we surmise that this is due to the low cell density in the modeled constructs (Ben-Or Frank et al. 2015), compared to the fully packed, and more in-vivo-like spatial arrangement of cells in our MSM framework here, which is also consistent with human fat histology studies (Guan et al. 2005; Sommer and Sattler 2000).

IF inclusions are dynamic energy storage depots that can be utilized during periods of elevated energy demand in active individuals and expand during periods of elevated lipid availability following food consumption and/or low energy expenditure. Specifically, IF tissue in trained individuals have improved metabolism, protecting them from insulin resistance. Sedentary obese individuals, on the other hand, have static IF tissue pools. Hence, elevated insulin secretion following consumption of processed carbohydrates promotes

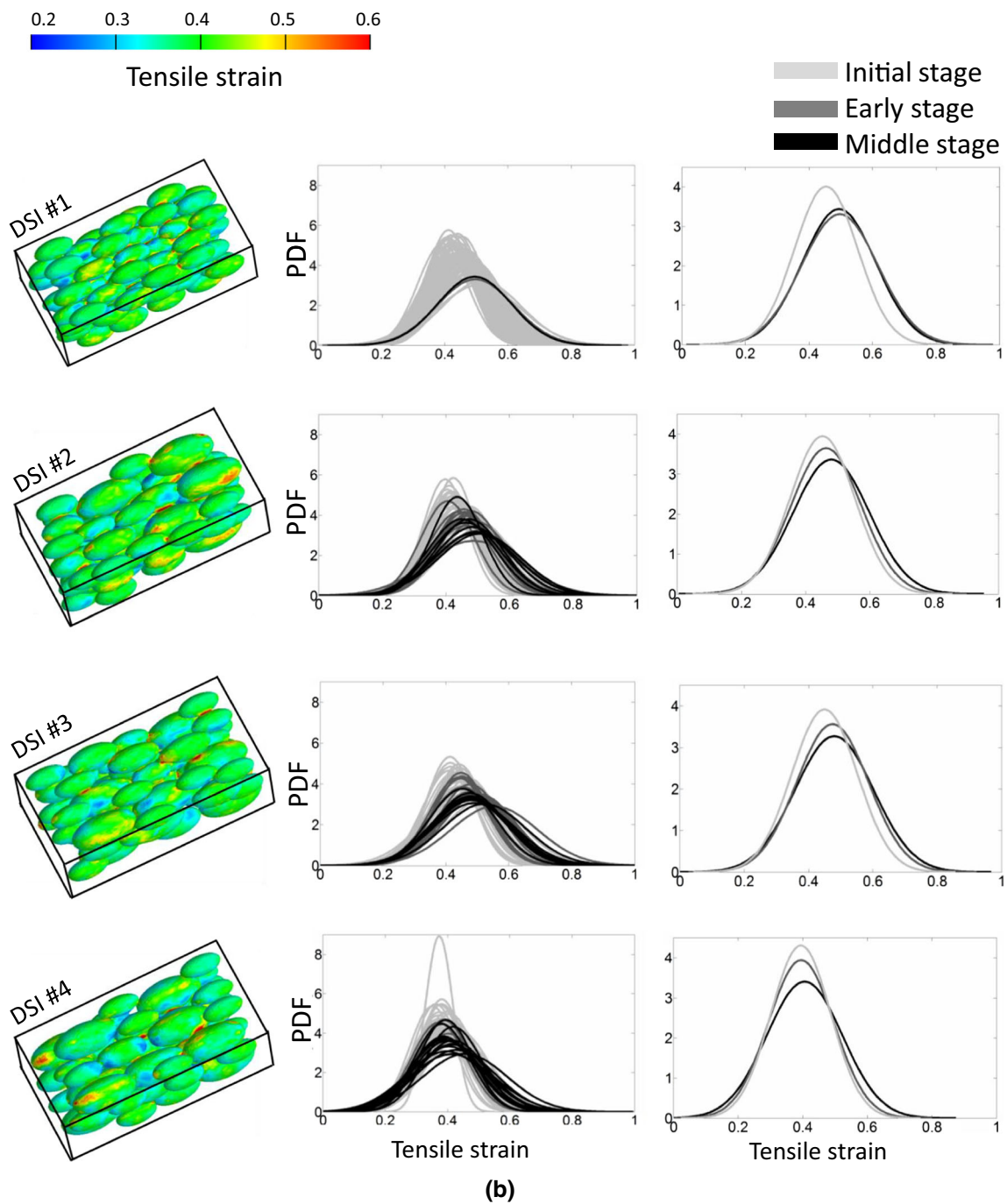


Fig. 8 continued

glucose oxidation, impairs fat oxidation, facilitates lipogenesis, and promotes storage of fat, while at the same time promoting insulin resistance, inflammation, and oxidative stress. The combination of insulin resistance and hyperinsulinemia further disrupts lipid metabolism. When dietary carbohydrate is restricted, however, metabolic processes shift to favor fat oxidation over lipid storage. Consequently, the lipid profile improves, and lipotoxic processes that impair β

cell function and insulin action resolve. Hence, consumption of high-fat diets in combination with adopting a sedentary lifestyle leads not only to the development of obesity but also to the development of metabolic impairments in skeletal muscle (e.g., insulin resistance) that contributes to whole-body disease states such as type-2 diabetes and cardiovascular diseases (Gower and Goss 2014; Shaw et al. 2010).

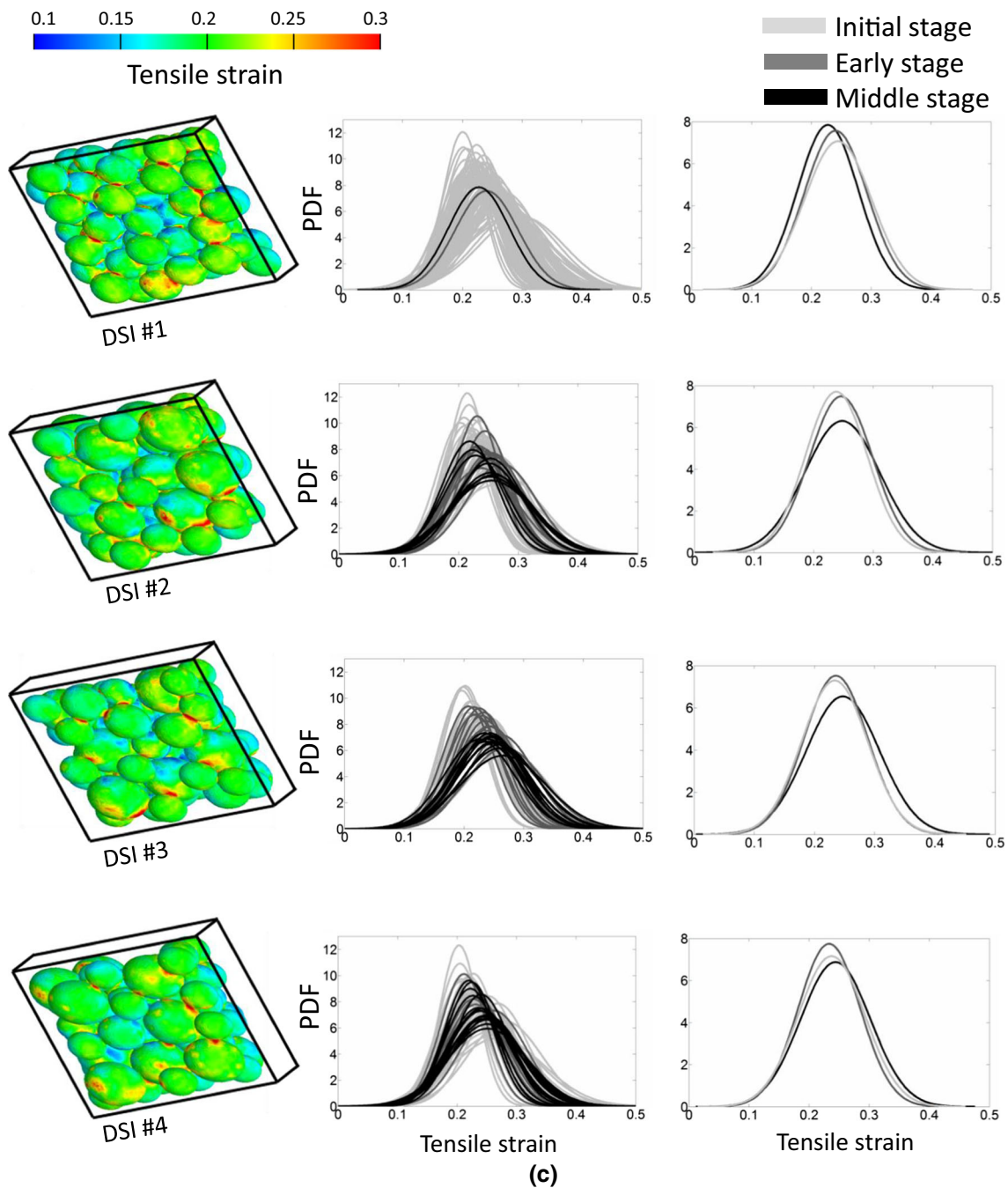
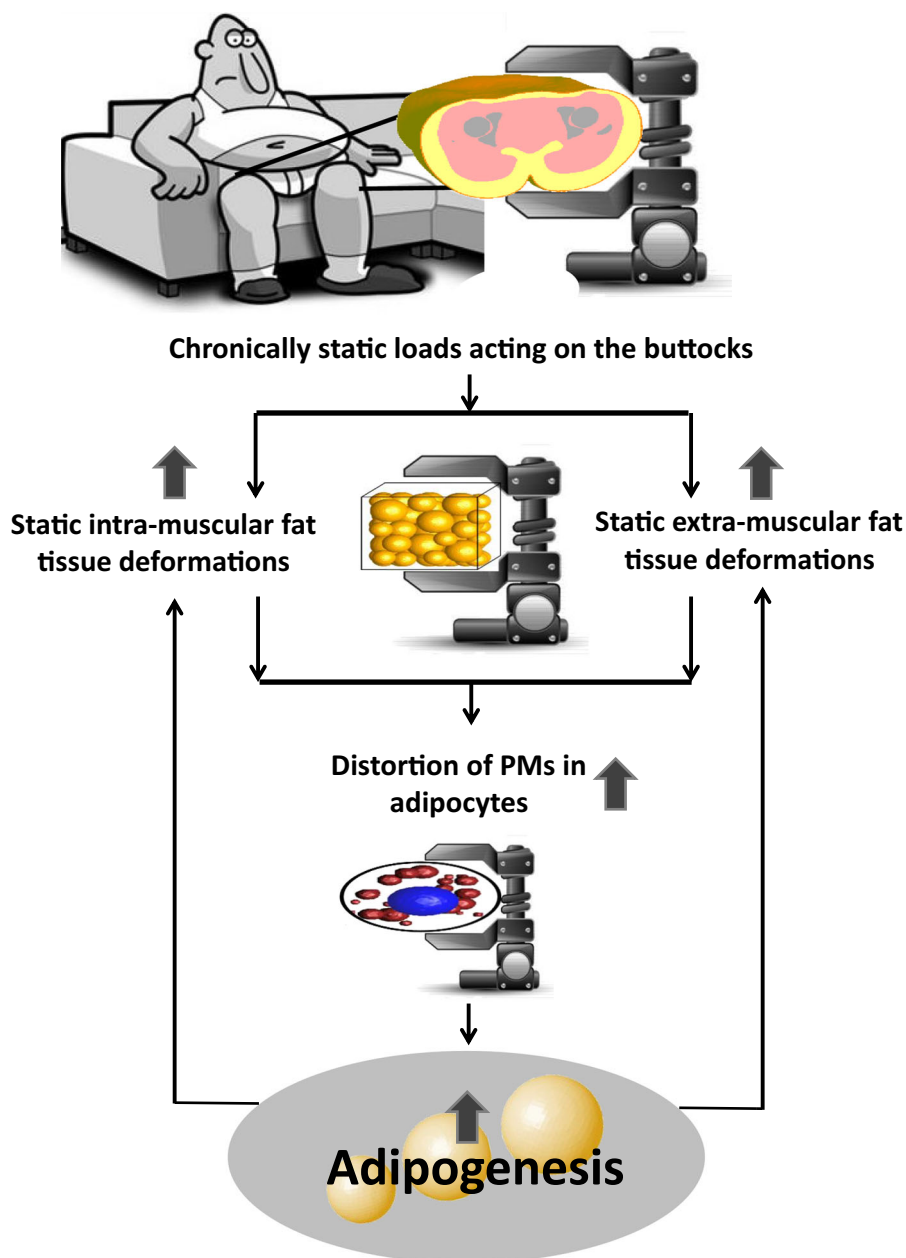


Fig. 8 continued

IF, much like the skeletal muscle tissues themselves, is generated continuously from MSCs which have several optional differentiation fates, two of them being to develop into adipocytes or myoblasts. A critical factor influencing the selection of a differentiation fate for MSCs is the mechanical environment that the MSCs sense, for example, in terms of stiffness of their surroundings and forces that apply (Gefen 2014; Li et al. 2013b; Santilli et al. 2014; Stenholm et al. 2008; Vettor et al. 2009; Watt and Huck 2013). With regard

to forces, it is important to emphasize that it is not only the magnitudes of the forces that are important in determining the fate of differentiation, but also the nature of application of the forces, particularly if the regime is dominantly static or dynamic (Gefen 2014; Santilli et al. 2014; Stenholm et al. 2008; Vettor et al. 2009). The nature of exposure of MSCs to external and body (e.g., gravity and muscle) forces is mostly static, which typically occurs in the elderly, but can also be the result of a sedentary lifestyle in young individuals. In a

Fig. 9 The proposed positive feedback loop which is contributing to the onset and development of sarcopenic obesity. When the buttocks is being loaded for long periods, static deformation in the muscle is accompanied by formation of intramuscular fat mass. Hence, distortion of the plasma membrane in adipocytes occurs both in the intramuscular and in the subcutaneous fat tissues. These elevated strains are very likely to stimulate additional adipogenesis, thereby increasing the content of lipid droplets at the cell scale and the mass of the fat tissues at the higher scales. These changes are expected to further enhance adipogenesis in a positive feedback loop, as so on and so forth



sedentary lifestyle, the MSCs will tend to commit to the adipogenic lineage, whereas dynamic force regimes will divert differentiation fates to bone and muscle cells (Benton et al. 2011; Gefen 2014; Goisser et al. 2015; Ivanovska et al. 2015; Parr et al. 2013; Shefer et al. 2010; Vettor et al. 2009). Clearly if more MSCs will differentiate into adipocytes—fat depots will eventually form and increase in size, both intramuscularly and extra-muscularly, which will then affect tissue loading states as explained previously. Some of the molecular mechanisms involved in the conversion of MSCs to fat cells include the PPARs and WNT growth factor pathways, which were found to be mechanically sensitive (Armstrong et al. 2007; Li et al. 2013a; Scarda et al. 2010; Sen et al. 2008;

Tu et al. 2012; Vettor et al. 2009). Overall, investigating the mechanical cues that trigger commitment to the adipogenic lineage, differentiation of adipocytes and production of intracellular lipids is highly important, especially since it could lead to knowledge regarding how to control IF contents and hence how to manage or treat sarcopenia.

The complexity of human biology and physiology exceeds by far what can be potentially described using a multiscale finite element model focusing on just the mechanobiology, as sophisticated as such modeling can be, because additional factors other than physical activity, including, for example, genetic and nutritional contributions, are involved as well. With that being said, the empirical association between

intramuscular fat and immobility is evident in the literature, particularly in the physiological and clinical literature (Elder et al. 2004; Gorgey and Shepherd 2010; Moore et al. 2015; Tuttle et al. 2011; Wroblewski et al. 2011; Leskinen et al. 2009; Manini et al. 2007; Addison et al. 2014). Elder et al. (2004), for example, performed a cross-sectional study and determined intramuscular fat levels in nonexercise-trained complete spinal cord-injured and nonexercise-trained nondisabled controls persons. They found an almost fourfold increase in intramuscular fat percentage in spinal cord injury (SCI) patients compared to nondisabled subjects. Consistently, Gorgey and Shepherd (2010) investigated the effects of neuromuscular electrical stimulation resistance training on individual muscle groups and adipose tissue of the right thigh in men with chronic SCI. They found a decrease of 50 % in the intramuscular fat following 12 weeks of biweekly training. More recently, Moore et al. (2015) found that the degree of fatty infiltration in skeletal muscle increased with the degree of the spinal injury. For example, participants with complete and incomplete SCI had 32 and 14 % lower muscle density values relative to their controls. They did find, however, variations in the degree of fatty infiltration between individuals with the same degree of injury, likely due to other factors such as genetics and nutrition.

When we transfer mechanical information between dimensional scales, we make a fundamental assumption regarding the required consistency of the tissue mechanical behavior between the macro- and micromodels. Treating the homogenized fat tissue properties at the buttocks and the extra cellular matrix in the cell constructs as being the same is one strategy we have adopted. The mechanical properties of the differentiating adipocytes do not disrupt this assumption, based on an analysis in a previous study published by our group (Shoham et al. 2013). Specifically, in Shoham et al. (2013) we have developed finite element models to examine the mechanical properties of three-dimensional tissue constructs containing adipocytes. Three model configurations were developed with different cell densities in each. The sizes of the adipocytes as well as the numbers and sizes of the intracellular lipid droplets were set according to our previously published empirical data. Mechanical properties were set according to the literature. The mechanical behavior (i.e., strain–stress curves) was documented while simulating a global compressive strain of up to 30 % to the volume of interest. Overall, we found that the stiffnesses of the constructs were mildly affected by the presence of the adipocytes. For example, in order to achieve a compressive strain of 30 % in the construct model without cells, there was a need to apply a compressive stress of 1.62 kPa, compared to 1.56 or 1.48 kPa in the volumes of interest which contained 3- and 5-adipocytes, respectively. In addition to that, in the multiscale approach used in our present study, we preserve the deformation tensor across the scales, thereby focusing on (cell/tissue

distortion) data that do not reflect the mechanical (stiffness) properties per se. The size of the cell-scale model was negligible compared to the whole buttocks model in our simulations. Hence, a first-order approximation was assumed to be sufficient. Other models might use second-order approximation for data exchange, i.e., using the deformation gradient and the deformation Laplacian, as was demonstrated by Erdemir et al. (2015) where cartilage and chondrocytes were simulated.

As in every computational modeling work, validation of the model against experimental data, which in turn reinforces the findings from the simulations, is critical. Here, we confirmed that the mechanical behavior of the simulated tissue blocks containing the highly packed adipocytes, under compression loading, agrees with reports of corresponding behavior of human subcutaneous adipose tissues (Alkhouli et al. 2013). On top of that, *in vivo* static mechanical stimulation of fat tissues was previously found to cause accelerated adipogenesis in mice models, where the enlarged fat mass was observed even after a single 2-h stimulation cycle (Heit et al. 2012; Kato et al. 2010; Lancerotto et al. 2013; Lujan-Hernandez et al. 2016). Moreover, the tissue changes that are characteristic to the buttocks of immobile patients, e.g., following a spinal cord injury, in which case fat tissues (and adipocytes) at the buttocks are being loaded statically, and subjected to sustained large deformations, include weight and fat mass gain as well as dominant fat infiltration into muscles (Gefen 2014; Gorgey and Dudley 2007). All of these tissue testing data, animal model experiments, and clinical reports strongly support the modeling, the findings, and the conclusions of the present study.

The multiscale simulations were conducted only for the reference macroscale model (at each location) due to numerical convergence problems related to the extremely high shear deformations which occur at the muscle–fat interfaces (due to the sharp tissue stiffness gradient) in the abnormally high fat infiltration model configurations. As a result of that, when we delivered the deformations that were developed in the intramuscular fat elements to the microscale models, the finite element numerical solution could not converge, even when using extremely dense meshes. The reference macroscale model elements of interest were chosen from the coronal plain—where the highest strain values were developed in fat tissues. In this plane, we have chosen three representative elements at different positions in the cross-sectional view. Eventually, we needed to make some practical compromises and hence considered elements with macroscale effective deformations that did not exceed 60 % due to the above-mentioned numerical convergence issues.

Potential obstructions to the vasculature in fat and muscle tissues due to weight-bearing or due to a cardiovascular disease or type-2 diabetes were not taken into account in the present MSM. Adequate perfusion is important for normal

metabolism in both fat and muscle (Linder-Ganz and Gefen 2007; Ruschkewitz and Gefen 2010, 2011; Shilo and Gefen 2012; Shoham and Gefen 2012a), and one could assume that with the gain of excessive fat tissue mass, cardiovascular impairments and/or diabetes may onset systemically, which would also contribute to the pathophysiology of fat gain. This concept is left for future multiphysics MSM research, which should consider that tissues subjected to sustained deformations could develop inflammation, or ischemic conditions, or both, which would in turn affect the mechanobiology of adipogenesis at all the dimensional scales. Moreover, sarcopenic obesity incorporates additional physiological pathologies which were not included in this model, e.g., increased subcutaneous fat mass or altered mechanical properties due to changes in tissue composition. Specifically, muscle tissues quickly lose strength as sarcopenic obesity develops, e.g., due to a decrease in fiber sizes and numbers and an intrinsic reduction in contractility in the intact fibers (Santilli et al. 2014; Stenholm et al. 2008). The purpose of this study was, however, to develop an innovative multiscale analysis platform and to focus on the mechanical contribution of intramuscular fat, where additional geometry and mechanical property changes are left for future studies. At the microscale, a more specific modeling of the PM of the cells along with the loaded receptors that trigger adipogenesis would be a great modeling tool.

In this study, we do not propose a specific threshold for the positive feedback loop nor a specific exercise protocol. Moreover, we are in doubt whether a universal threshold value or protocol actually exist, particularly given the inter-subject variability driven by gender, age, genetics, and health conditions, and possibly nutrition and lifestyle. Rather than proposing specific numbers, the main contribution of our present work is in the new mechanical perspective to study the mechanobiology of fat and in particular, of sarcopenic obesity and the mechanotransduction processes which it involves, that were not taken into account in previous studies of the disease.

To summarize, here we presented the first MSM of fat tissues and have demonstrated that adipocytes in weight-bearing adipose tissues could be triggered to differentiate by mechanical stimuli in a positive feedback loop. Our outcomes are highly relevant in research adipose-related diseases since mechanical distortion of adipocytes trigger adipogenesis and fat gain at the different dimensional scales. This novel concept should be taken into account when establishing prevention strategies and treatments for sarcopenic obesity and related diseases.

Acknowledgements This research work was supported by grants from the Israel Science Foundation (Nos. 611/12 and 1266/16, A.G. and D.B.).

Conflict of interest The authors declare that they have no conflict of interest.

References

- Addison O, Marcus RL, Lastayo PC, Ryan AS (2014) Intermuscular fat: a review of the consequences and causes. *Int J Endocrinol* 2014:309570
- Albu JB, Kenya S, He Q, Wainwright M, Berk ES, Heshka S, Kotler DP, Engelson ES (2007) Independent associations of insulin resistance with high whole-body intermuscular and low leg subcutaneous adipose tissue distribution in obese HIV-infected women. *Am J Clin Nutr* 86:100–106
- Albu JB, Kovera AJ, Allen L, Wainwright M, Berk E, Raja-Khan N, Janumala I, Burkey B, Heshka S, Gallagher D (2005) Independent association of insulin resistance with larger amounts of intermuscular adipose tissue and a greater acute insulin response to glucose in African American than in white nondiabetic women. *Am J Clin Nutr* 82:1210–1217
- Alkhouli N, Mansfield J, Green E, Bell J, Knight B, Liversedge N, Tham JC, Welbourn R, Shore AC, Kos K, Winlove CP (2013) The mechanical properties of human adipose tissues and their relationships to the structure and composition of the extracellular matrix. *Am J Physiol Endocrinol Metab* 305:E1427–E1435
- Armstrong VJ, Muzylak M, Sunters A, Zaman G, Saxon LK, Price JS, Lanyon LE (2007) Wnt/beta-catenin signaling is a component of osteoblastic bone cell early responses to load-bearing and requires estrogen receptor alpha. *J Biol Chem* 282:20715–20727
- Barkaoui A, Chamekh A, Merzouki T, Hambl R, Mkaddem A (2014) Multiscale approach including microfibril scale to assess elastic constants of cortical bone based on neural network computation and homogenization method. *Int J Numer Method Biomed Eng* 30:318–338
- Ben-Or Frank M, Shoham N, Benayahu D, Gefen A (2015) Effects of accumulation of lipid droplets on load transfer between and within adipocytes. *Biomech Model Mechanobiol* 14:15–28
- Benton MJ, Whyte MD, Dyal BW (2011) Sarcopenic obesity: strategies for management. *Am J Nurs* 111:38–44 quiz 45-6
- Case N, Thomas J, Xie Z, Sen B, Styner M, Rowe D, Rubin J (2013) Mechanical input restrains PPAR γ 2 expression and action to preserve mesenchymal stem cell multipotentiality. *Bone* 52:454–464
- Colloca M, Blanchard R, Hellmich C, Ito K, van Rietbergen B (2014) A multiscale analytical approach for bone remodeling simulations: linking scales from collagen to trabeculae. *Bone* 64:303–313
- Delaine-Smith RM, Reilly GC (2012) Mesenchymal stem cell responses to mechanical stimuli. *Muscles Ligaments Tendons J* 2:169–180
- Elder CP, Apple DF, Bickel CS, Meyer RA, Dudley GA (2004) Intramuscular fat and glucose tolerance after spinal cord injury—a cross-sectional study. *Spinal Cord* 42:711–716
- Elsner JJ, Gefen A (2008) Is obesity a risk factor for deep tissue injury in patients with spinal cord injury? *J Biomech* 41:3322–3331
- Erdemir A, Bennetts C, Davis S, Reddy A, Sibole S (2015) Multiscale cartilage biomechanics: technical challenges in realizing a high-throughput modelling and simulation workflow. *Interface Focus* 5:20140081
- Finkelstein EA, Khavjou OA, Thompson H, Trogon JG, Pan L, Sherry B, Dietz W (2012) Obesity and severe obesity forecasts through 2030. *Am J Prev Med* 42:563–570
- Gefen A, Weihs D (2016) Cytoskeleton and plasma-membrane damage resulting from exposure to sustained deformations: A review of the mechanobiology of chronic wounds. *Med Eng Phys*. doi:10.1016/j.medengphy.2016.05.014
- Gefen A (2014) Tissue changes in patients following spinal cord injury and implications for wheelchair cushions and tissue loading: a literature review. *Ostomy Wound Manage* 60:34–45

- Goisser S, Kemmler W, Porzel S, Volkert D, Sieber CC, Bollheimer LC, Freiburger E (2015) Sarcopenic obesity and complex interactions with nutrition and exercise in community-dwelling older persons—a narrative review. *Clin Interv Aging* 10:1267–1282
- Goodpaster BH, Krishnaswami S, Harris TB, Katsiaras A, Kritchevsky SB, Simonsick EM, Nevitt M, Holvoet P, Newman AB (2005) Obesity, regional body fat distribution, and the metabolic syndrome in older men and women. *Arch Intern Med* 165:777–783
- Goodpaster BH, Thaete FL, Kelley DE (2000) Thigh adipose tissue distribution is associated with insulin resistance in obesity and in type 2 diabetes mellitus. *Am J Clin Nutr* 71:885–892
- Gorgey AS, Dudley GA (2007) Skeletal muscle atrophy and increased intramuscular fat after incomplete spinal cord injury. *Spinal Cord* 45:304–309
- Gorgey AS, Shepherd C (2010) Skeletal muscle hypertrophy and decreased intramuscular fat after unilateral resistance training in spinal cord injury: case report. *J Spinal Cord Med* 33:90–95
- Granneman JG, Li P, Lu Y, Tilak J (2004) Seeing the trees in the forest: selective electroporation of adipocytes within adipose tissue. *Am J Physiol Endocrinol Metab* 287:E574–E582
- Guan H, Arany E, van Beek JP, Chamson-Reig A, Thyssen S, Hill DJ, Yang K (2005) Adipose tissue gene expression profiling reveals distinct molecular pathways that define visceral adiposity in offspring of maternal protein-restricted rats. *Am J Physiol Endocrinol Metab* 288:E663–E673
- Hambli R, Katerchi H, Benhamou CL (2011) Multiscale methodology for bone remodelling simulation using coupled finite element and neural network computation. *Biomech Model Mechanobiol* 10:133–145
- Hartmann D (2010) A multiscale model for red blood cell mechanics. *Biomech Model Mechanobiol* 9:1–17
- Hayenga HN, Thorne BC, Peirce SM, Humphrey JD (2011) Ensuring congruency in multiscale modeling: towards linking agent based and continuum biomechanical models of arterial adaptation. *Ann Biomed Eng* 39:2669–2682
- Heit YI, Lancerotto L, Mesteri I, Ackermann M, Navarrete MF, Nguyen CT, Mukundan S Jr, Konerding MA, Del Vecchio DA, Orgill DP (2012) External volume expansion increases subcutaneous thickness, cell proliferation, and vascular remodeling in a murine model. *Plast Reconstr Surg* 130:541–547
- Ivanovska IL, Shin JW, Swift J, Discher DE (2015) Stem cell mechanobiology: diverse lessons from bone marrow. *Trends Cell Biol* 25:523–532
- Kato H, Suga H, Eto H, Araki J, Aoi N, Doi K, Iida T, Tabata Y, Yoshimura K (2010) Reversible adipose tissue enlargement induced by external tissue suspension: possible contribution of basic fibroblast growth factor in the preservation of enlarged tissue. *Tissue Eng Part A* 16:2029–2040
- Katzengold R, Shoham N, Benayahu D, Gefen A (2015) Simulating single cell experiments in mechanical testing of adipocytes. *Biomech Model Mechanobiol* 14:537–547
- Khoury RK, Schlenz I, Murphy BJ, Baker TJ (2000) Nonsurgical breast enlargement using an external soft-tissue expansion system. *Plast Reconstr Surg* 105:2500–2512 (discussion 2513–4)
- Krishnamoorthy D, Frechette DM, Adler BJ, Green DE, Chan ME, Rubin CT (2016) Marrow adipogenesis and bone loss that parallels estrogen deficiency is slowed by low-intensity mechanical signals. *Osteoporos Int* 27:747–756
- Lancerotto L, Chin MS, Freniere B, Lujan-Hernandez JR, Li Q, Valderama Vasquez A, Bassetto F, Del Vecchio DA, Lalikos JF, Orgill DP (2013) Mechanisms of action of external volume expansion devices. *Plast Reconstr Surg* 132:569–578
- Leskinen T, Sipilä S, Alen M, Cheng S, Pietiläinen KH, Usenius JP, Suominen H, Kovanen V, Kainulainen H, Kaprio J, Kujala UM (2009) Leisure-time physical activity and high-risk fat: a longitudinal population-based twin study. *Int J Obes (Lond)* 33:1211–1218
- Levy A, Enzer S, Shoham N, Zaretsky U, Gefen A (2012) Large, but not small sustained tensile strains stimulate adipogenesis in culture. *Ann Biomed Eng* 40:1052–1060
- Levy A, Kopplin K, Gefen A (2014) An air-cell-based cushion for pressure ulcer protection remarkably reduces tissue stresses in the seated buttocks with respect to foams: finite element studies. *J Tissue Viability* 23:13–23
- Levy A, Kopplin K, Gefen A (2013) Simulations of skin and subcutaneous tissue loading in the buttocks while regaining weight-bearing after a push-up in wheelchair users. *J Mech Behav Biomed Mater* 28:436–447
- Li G, Fu N, Yang X, Li M, Ba K, Wei X, Fu Y, Yao Y, Cai X, Lin Y (2013) Mechanical compressive force inhibits adipogenesis of adipose stem cells. *Cell Prolif* 46:586–594
- Li R, Liang L, Dou Y, Huang Z, Mo H, Wang Y, Yu B (2015) Mechanical strain regulates osteogenic and adipogenic differentiation of bone marrow mesenchymal stem cells. *Biomed Res Int* 2015:873251
- Li Z, Gong Y, Sun S, Du Y, Lü D, Liu X, Long M (2013) Differential regulation of stiffness, topography, and dimension of substrates in rat mesenchymal stem cells. *Biomaterials* 34:7616–7625
- Linder-Ganz E, Gefen A (2004) Mechanical compression-induced pressure sores in rat hindlimb: muscle stiffness, histology, and computational models. *J Appl Physiol* (1985) 96:2034–2049
- Linder-Ganz E, Gefen A (2007) The effects of pressure and shear on capillary closure in the microstructure of skeletal muscles. *Ann Biomed Eng* 35:2095–2107
- Lujan-Hernandez J, Lancerotto L, Nabzyk C, Hassan KZ, Giatsidis G, Khouri RK Jr, Chin MS, Bassetto F, Lalikos JF, Orgill DP (2016) Induction of adipogenesis by external volume expansion. *Plast Reconstr Surg* 137:122–131
- Luu YK, Capilla E, Rosen CJ, Gilsanz V, Pessin JE, Judex S, Rubin CT (2009) Mechanical stimulation of mesenchymal stem cell proliferation and differentiation promotes osteogenesis while preventing dietary-induced obesity. *J Bone Miner Res* 24:50–61
- Manini TM, Clark BC, Nalls MA, Goodpaster BH, Ploutz-Snyder LL, Harris TB (2007) Reduced physical activity increases intermuscular adipose tissue in healthy young adults. *Am J Clin Nutr* 85:377–384
- Monteiro R, Azevedo I (2010) Chronic inflammation in obesity and the metabolic syndrome. *Mediators Inflamm* 2010:289645
- Moo EK, Herzog W, Han SK, Abu Osman NA, Pingguan-Murphy B, Federico S (2012) Mechanical behaviour of in-situ chondrocytes subjected to different loading rates: a finite element study. *Biomech Model Mechanobiol* 11:983–993
- Moore CD, Craven BC, Thabane L, Laing AC, Frank-Wilson AW, Kontulainen SA, Papaioannou A, Adachi JD, Giangregorio LM (2015) Lower-extremity muscle atrophy and fat infiltration after chronic spinal cord injury. *J Musculoskelet Neuronal Interact* 15:32–41
- Oomens CW, Zenhorst W, Broek M, Hemmes B, Poeze M, Brink PR, Bader DL (2013) A numerical study to analyse the risk for pressure ulcer development on a spine board. *Clin Biomech (Bristol, Avon)* 28:736–742
- Or-Tzadikario S, Gefen A (2011) Confocal-based cell-specific finite element modeling extended to study variable cell shapes and intracellular structures: the example of the adipocyte. *J Biomech* 44:567–573
- Parr EB, Coffey VG, Hawley JA (2013) ‘Sarcobesity’: a metabolic conundrum. *Maturitas* 74:109–113
- Reese SP, Ellis BJ, Weiss JA (2013) Multiscale modeling of ligaments and tendons. In: Gefen A (ed) *Multiscale computer modeling in biomechanics and biomedical engineering*. Springer, Berlin, pp 103–147
- Reese SP, Ellis BJ, Weiss JA (2013) Micromechanical model of a surrogate for collagenous soft tissues: development, validation and analysis of mesoscale size effects. *Biomech Model Mechanobiol* 12:1195–1204

- Robles PG, Sussman MS, Naraghi A, Brooks D, Goldstein RS, White LM, Mathur S (2015) Intramuscular fat infiltration contributes to impaired muscle function in COPD. *Med Sci Sports Exerc* 47:1334–1341
- Roubenoff R (2004) Sarcopenic obesity: the confluence of two epidemics. *Obes Res* 12:887–888
- Rubin CT, Capilla E, Luu YK, Busa B, Crawford H, Nolan DJ, Mittal V, Rosen CJ, Pessin JE, Judex S (2007) Adipogenesis is inhibited by brief, daily exposure to high-frequency, extremely low-magnitude mechanical signals. *Proc Natl Acad Sci USA* 104:17879–17884
- Ruschkewitz Y, Gefen A (2010) Cell-level temperature distributions in skeletal muscle post spinal cord injury as related to deep tissue injury. *Med Biol Eng Comput* 48:113–122
- Ruschkewitz Y, Gefen A (2011) Cellular-scale transport in deformed skeletal muscle following spinal cord injury. *Comput Methods Biomech Biomed Eng* 14:411–424
- Santilli V, Bernetti A, Mangone M, Paoloni M (2014) Clinical definition of sarcopenia. *Clin Cases Miner Bone Metab* 11:177–180
- Scarda A, Franzin C, Milan G, Sanna M, Dal Prà C, Pagano C, Boldrin L, Piccoli M, Trevelin E, Granzotto M, Gamba P, Federspil G, De Coppi P, Vettor R (2010) Increased adipogenic conversion of muscle satellite cells in obese Zucker rats. *Int J Obes (Lond)* 34:1319–1327
- Sen B, Xie Z, Case N, Ma M, Rubin C, Rubin J (2008) Mechanical strain inhibits adipogenesis in mesenchymal stem cells by stimulating a durable beta-catenin signal. *Endocrinology* 149:6065–6075
- Shaw CS, Clark J, Wagenmakers AJ (2010) The effect of exercise and nutrition on intramuscular fat metabolism and insulin sensitivity. *Annu Rev Nutr* 30:13–34
- Shefer G, Rauner G, Yablonka-Reuveni Z, Benayahu D (2010) Reduced satellite cell numbers and myogenic capacity in aging can be alleviated by endurance exercise. *PLoS One* 5:e13307
- Shilo M, Gefen A (2012) Identification of capillary blood pressure levels at which capillary collapse is likely in a tissue subjected to large compressive and shear deformations. *Comput Methods Biomech Biomed Engin* 15:59–71
- Shoham N, Gefen A (2012a) Deformations, mechanical strains and stresses across the different hierarchical scales in weight-bearing soft tissues. *J Tissue Viability* 21:39–46
- Shoham N, Gefen A (2012b) Mechanotransduction in adipocytes. *J Biomech* 45:1–8
- Shoham N, Gefen A (2011) Stochastic modeling of adipogenesis in 3T3-L1 cultures to determine probabilities of events in the cell's life cycle. *Ann Biomed Eng* 39:2637–2653
- Shoham N, Girshovitz P, Katzungold R, Shaked NT, Benayahu D, Gefen A (2014) Adipocyte stiffness increases with accumulation of lipid droplets. *Biophys J* 106:1421–1431
- Shoham N, Gottlieb R, Sharabani-Yosef O, Zaretsky U, Benayahu D, Gefen A (2012) Static mechanical stretching accelerates lipid production in 3T3-L1 adipocytes by activating the MEK signaling pathway. *Am J Physiol Cell Physiol* 302:C429–C441
- Shoham N, Levy A, Kopplin K, Gefen A (2015a) Contoured foam cushions cannot provide long-term protection against pressure-ulcers for individuals with a spinal cord injury: modeling studies. *Adv Skin Wound Care* 28:303–316
- Shoham N, Mor-Yossef Moldovan L, Benayahu D (2015b) Multiscale modeling of tissue-engineered fat: is there a deformation-driven positive feedback loop in adipogenesis? *Tissue Eng Part A* 21:1354–63
- Shoham N, Sasson AL, Lin FH, Benayahu D, Haj-Ali R, Gefen A (2013) The mechanics of hyaluronic acid/adipic acid dihydrazide hydrogel: towards developing a vessel for delivery of preadipocytes to native tissues. *J Mech Behav Biomed Mater* 28:320–331
- Sibole SC, Erdemir A (2012) Chondrocyte deformations as a function of tibiofemoral joint loading predicted by a generalized high-throughput pipeline of multi-scale simulations. *PLoS One* 7:e37538
- Sibole SC, Maas S, Halloran JP, Weiss JA, Erdemir A (2013) Evaluation of a post-processing approach for multiscale analysis of biphasic mechanics of chondrocytes. *Comput Methods Biomech Biomed Eng* 16:1112–1126
- Sommer B, Sattler G (2000) Current concepts of fat graft survival: histology of aspirated adipose tissue and review of the literature. *Dermatol Surg* 26:1159–1166
- Sopher R, Nixon J, Gorecki C, Gefen A (2011) Effects of intramuscular fat infiltration, scarring, and spasticity on the risk for sitting-acquired deep tissue injury in spinal cord injury patients. *J Biomech Eng* 133:021011
- Stenholm S, Harris TB, Rantanen T, Visser M, Kritchevsky SB, Ferrucci L (2008) Sarcopenic obesity: definition, cause and consequences. *Curr Opin Clin Nutr Metab Care* 11:693–700
- Tanabe Y, Koga M, Saito M, Matsunaga Y, Nakayama K (2004) Inhibition of adipocyte differentiation by mechanical stretching through ERK-mediated downregulation of PPARgamma2. *J Cell Sci* 117:3605–3614
- Tanska P, Mononen ME, Korhonen RK (2015) A multi-scale finite element model for investigation of chondrocyte mechanics in normal and medial meniscectomy human knee joint during walking. *J Biomech* 48:1397–1406
- Tu X, Rhee Y, Condon KW, Bivi N, Allen MR, Dwyer D, Stolina M, Turner CH, Robling AG, Plotkin LI, Bellido T (2012) Sost down-regulation and local Wnt signaling are required for the osteogenic response to mechanical loading. *Bone* 50:209–217
- Turner NJ, Jones HS, Davies JE, Canfield AE (2008) Cyclic stretch-induced TGFbeta1/Smad signaling inhibits adipogenesis in umbilical cord progenitor cells. *Biochem Biophys Res Commun* 377:1147–1151
- Tuttle LJ, Sinacore DR, Cade WT, Mueller MJ (2011) Lower physical activity is associated with higher intermuscular adipose tissue in people with type 2 diabetes and peripheral neuropathy. *Phys Ther* 91:923–930
- Velloso CP (2008) Regulation of muscle mass by growth hormone and IGF-I. *Br J Pharmacol* 154:557–568
- Verstraeten VL, Renes J, Ramaekers FC, Kamps M, Kuijpers HJ, Verheyen F, Wabitsch M, Steijlen PM, van Steensel MA, Broers JL (2011) Reorganization of the nuclear lamina and cytoskeleton in adipogenesis. *Histochem Cell Biol* 135:251–261
- Vettor R, Milan G, Franzin C, Sanna M, De Coppi P, Rizzuto R, Federspil G (2009) The origin of intermuscular adipose tissue and its pathophysiological implications. *Am J Physiol Endocrinol Metab* 297:E987–E998
- Watt FM, Huck WT (2013) Role of the extracellular matrix in regulating stem cell fate. *Nat Rev Mol Cell Biol* 14:467–473
- Wroblewski AP, Amati F, Smiley MA, Goodpaster B, Wright V (2011) Chronic exercise preserves lean muscle mass in masters athletes. *Phys Sportsmed* 39:172–178
- Yang X, Cai X, Wang J, Tang H, Yuan Q, Gong P, Lin Y (2012) Mechanical stretch inhibits adipogenesis and stimulates osteogenesis of adipose stem cells. *Cell Prolif* 45:158–166
- Yim JE, Heshka S, Albu J, Heymsfield S, Kuznia P, Harris T, Gallagher D (2007) Intermuscular adipose tissue rivals visceral adipose tissue in independent associations with cardiovascular risk. *Int J Obes (Lond)* 31:1400–1405
- Yim JE, Heshka S, Albu JB, Heymsfield S, Gallagher D (2008) Femoral-gluteal subcutaneous and intermuscular adipose tissues have independent and opposing relationships with CVD risk. *J Appl Physiol* (1985) 104:700–707
- Zamboni M, Mazzali G, Fantin F, Rossi A, Di Francesco V (2008) Sarcopenic obesity: a new category of obesity in the elderly. *Nutr Metab Cardiovasc Dis* 18:388–395